

AZIMUTHAL ANGLES IN DIFFRACTIVE ep COLLISIONS

M. Diehl¹

Centre de Physique Théorique²
Ecole Polytechnique
91128 Palaiseau Cedex, France
and

Department of Applied Mathematics and Theoretical Physics
University of Cambridge
Cambridge CB3 9EW, England

Abstract

We investigate azimuthal correlations in deep inelastic diffractive scattering, $e + p \rightarrow e + \tilde{p} + X$. The dependence of the ep cross section on the angle between the lepton plane and some direction in the hadronic final state can be written in a simple form; its measurement can be used to constrain the cross section for longitudinally polarised photons. Using the model of nonperturbative two-gluon exchange of Landshoff and Nachtmann we calculate the distribution of the azimuthal jet angle in diffractive dijet production and find that useful bounds on the longitudinal cross section for such events might be obtained from its measurement. We then discuss the predictions of this model for the dependence of the ep cross section on the azimuthal angle of the proton remnant \tilde{p} , which contains information about the helicity content of the pomeron.

¹email: diehl@orphee.polytechnique.fr

²Unité propre 14 du CNRS

1 Introduction

Our knowledge of diffractive physics in deep inelastic electron-proton scattering is greatly increasing as diffractive events are being studied in more and more detail at HERA [1]. The phenomenology of these events has many aspects, and several theoretical models have been proposed to describe them [2, 3, 4, 5, 6, 7, 8]. Despite various successes of these models we are yet far from a clear theoretical picture of what pomeron physics is in terms of QCD. Detailed studies of the characteristics of the final state might help to further our understanding of the underlying mechanisms and to distinguish between various models.

The measurement of two different kinds of azimuthal angles has recently been proposed: the azimuthal angle of the scattered proton [9, 10] or, equivalently, of the diffractive system as a whole, and the azimuthal angle of the jets in events with only two jets of large transverse momentum in the diffractive final state [11]. The present paper will be concerned with both issues and has two purposes: to discuss some general aspects of azimuthal distributions in diffraction and to present in detail predictions for such distributions in the model of nonperturbative two-gluon exchange of Landshoff and Nachtmann [12].

The structure of this paper is as follows. In sec. 2 we generalise the formalism of [9] for azimuthal distributions in diffraction and show which constraints on the γ^*p cross section for longitudinal photons their measurement can provide. A corresponding framework has long been used in various processes in non-diffractive DIS [13, 14]. As an application we consider in sec. 3 the azimuthal angle of the jets in diffractive dijet production. Some features of its distribution are quite characteristic for two-gluon exchange and might offer a way to test the two-gluon approximation in this type of events as was already pointed out in [11]. We calculate the angular dependence in the Landshoff-Nachtmann model and show which bounds on the longitudinal cross sections could be obtained from its measurement. We also show how this method can be generalised to final states that do not necessarily have two-jet topology. In sec. 4 we generalise the calculation to nonzero t and obtain the corrections this gives for the γ^*p cross sections and for the distribution of the azimuthal jet angle. Using this calculation we investigate a genuine finite- t effect in sec. 5: the correlation between the azimuthal angles of the scattered lepton and proton. In [9] it was shown that this observable contains information about the helicity structure of the pomeron and argued that it might provide a sensitive test of various theoretical ideas about the underlying dynamics. We conclude with a summary in sec. 6.

2 Azimuthal angle dependence in diffraction

We begin by extending the formalism of [9] to a large class of azimuthal angles in diffractive electron-proton or positron-proton collisions,

$$e(k) + p(p) \rightarrow e(k') + \tilde{p}(\tilde{p}) + X(p_X) , \quad (2.1)$$

where the proton remnant \tilde{p} can be a proton or a diffractive excitation of a proton and where four-momenta are indicated in parentheses. We will use the conventional kinematic quantities Q^2, W^2, x, y, s, t for deep inelastic scattering, M_X for the invariant mass of the diffractive system X , and the variables $\beta = Q^2/(Q^2 + M_X^2 - t)$ and $\xi = (Q^2 + M_X^2 - t)/(W^2 + Q^2 - m_p^2)$.

Working in the γ^*p rest frame one can write the azimuthal dependence of the ep cross section in a simple way by making use of the factorisation of (2.1) into γ^* emission by the electron or positron and a diffractive photon-proton collision

$$\gamma^*(q) + p(p) \rightarrow X(p_X) + \tilde{p}(\tilde{p}) . \quad (2.2)$$

To achieve this it is essential that the selection of diffractive events, e.g. the definition of a rapidity gap between X and \tilde{p} , is unaffected by a common rotation about the γ^*p axis of the momenta in the hadronic final state $X\tilde{p}$, with the lepton momenta k and k' being kept fixed. This is guaranteed if the selection criteria only involve quantities of the γ^*p reaction, i.e. if they do *not* refer to the lepton momenta k and k' . Examples for such criteria have been given in [9].

We define an azimuthal angle with respect to a direction in the hadronic final state $X\tilde{p}$. To this end we introduce a four-vector h which depends only on particle momenta in the γ^*p reaction (2.2), i.e. on p, q and the momenta of the final state hadrons. Using a right-handed Cartesian coordinate system with the z axis in the direction of the photon momentum \mathbf{q} and some fixed x and y axes we define φ as the azimuthal angle between the lepton momentum \mathbf{k} and the vector \mathbf{h} , i.e. as the azimuthal angle of \mathbf{k} minus the azimuthal angle of \mathbf{h} .

We also use h to introduce polarisation vectors for the virtual photon:

$$\varepsilon_0 = \frac{1}{Q\sqrt{1 + m_p^2 Q^2/(p \cdot q)^2}} \left(q + \frac{Q^2}{p \cdot q} p \right) , \quad \varepsilon_1 = \frac{h_T}{\sqrt{-h_T^2}} , \quad \varepsilon_2 = \frac{n}{\sqrt{-n^2}} , \quad (2.3)$$

where

$$h_T = h - \frac{(p \cdot q)(p \cdot h) - m_p^2(q \cdot h)}{(p \cdot q)^2 + m_p^2 Q^2} q - \frac{(p \cdot q)(q \cdot h) + Q^2(p \cdot h)}{(p \cdot q)^2 + m_p^2 Q^2} p \quad (2.4)$$

is the transverse part of h with respect to p and q , and $n^\mu = \varepsilon^{\mu\nu\rho\sigma} p_\nu q_\rho h_\sigma$ is normal to p, q and h . Polarisation for positive or negative photon helicity are as usual given by $\varepsilon_\pm = \mp(\varepsilon_1 \pm i\varepsilon_2)/\sqrt{2}$.

The contractions of $\varepsilon_-^\mu, \varepsilon_0^\mu, \varepsilon_+^\mu$ with the appropriate matrix element of the hadronic electromagnetic current eJ_μ give the amplitudes $e\mathcal{M}_m$ for subreaction (2.2) with photon helicity m ,

$$e\mathcal{M}_m = \langle X\tilde{p} \text{ out} | eJ_\mu(0) | p \rangle \cdot \varepsilon_m^\mu , \quad m = -, 0, + . \quad (2.5)$$

The corresponding differential cross sections $d\sigma_{mm}$ are obtained by multiplying $\mathcal{M}_m^* \mathcal{M}_m$ with the phase space element of the hadronic final state $X\tilde{p}$ and with a normalisation factor, summing over the states $X\tilde{p}$ allowed by our selection criteria for the diffractive reaction and averaging over the initial proton spin. Our normalisation factor corresponds to Hand's convention [15] for the photon flux. From $\mathcal{M}_m^* \mathcal{M}_n$ with $m \neq n$ we define in an analogous manner differential interference terms $d\sigma_{mn}$ between photons with helicities m and n . It is easy to see that the matrix $d\sigma_{mn}$ is hermitian, $d\sigma_{mn} = d\sigma_{nm}^*$.

With the requirement on the selection cuts formulated above the $d\sigma_{mn}$ are invariant under a common rotation of the momenta in the hadronic final state $X\tilde{p}$ about the γ^*p axis. This is because our transverse photon polarisations are not fixed but vary with the final state as they depend on h . One can show that the cross sections $d\sigma_{mm}$ are the same for different choices of this vector, whereas the interference terms are not. In the following sections we will put extra labels on the angle φ and the $d\sigma_{mn}$ to distinguish different choices of h , though for the diagonals $d\sigma_{mm}$ this would not be necessary.

Integrating over the phase space of the hadronic final state we obtain a matrix σ_{mn} . We will also consider γ^*p cross sections and interference terms that are differential in some kinematical variables of the final state, such as the momentum of the proton remnant or internal variables of the system X . We will only use variables that can be defined as Lorentz invariant functions of the four-momenta in the γ^*p reaction. Provided that the selection criteria for our reaction do not refer to any particular frame, the differential cross sections and interference terms are then Lorentz invariant and as a consequence depend only on W^2 , Q^2 and the variables in which they are differential. Due to the rotation invariance property just mentioned they are independent of the azimuthal angle of \mathbf{h} in our fixed coordinate system and hence also of φ . An important property following from angular momentum conservation is that interference terms which are differential in the direction of h vanish when h becomes collinear with q and p , in which case the azimuthal angle φ is undefined [9].

The ep cross section can now be written as [9]

$$\begin{aligned} \frac{d\sigma(ep \rightarrow e\tilde{p}X)}{dx dQ^2 d\varphi} = & \frac{2\tilde{\Gamma}}{2\pi} \left\{ \frac{1}{2}(\sigma_{++} + \sigma_{--}) + \varepsilon\sigma_{00} \right. \\ & - \varepsilon \cos(2\varphi) \operatorname{Re} \sigma_{+-} + \varepsilon \sin(2\varphi) \operatorname{Im} \sigma_{+-} \\ & - \sqrt{\varepsilon(1+\varepsilon)} \cos \varphi \operatorname{Re} (\sigma_{+0} - \sigma_{-0}) \\ & + \sqrt{\varepsilon(1+\varepsilon)} \sin \varphi \operatorname{Im} (\sigma_{+0} + \sigma_{-0}) \\ & + r_L \sqrt{1-\varepsilon^2} \frac{1}{2}(\sigma_{++} - \sigma_{--}) \\ & \left. - r_L \sqrt{\varepsilon(1-\varepsilon)} \cos \varphi \operatorname{Re} (\sigma_{+0} + \sigma_{-0}) \right\} \end{aligned}$$

$$+ r_L \sqrt{\varepsilon(1-\varepsilon)} \sin \varphi \operatorname{Im}(\sigma_{+0} - \sigma_{-0}) \Big\} , \quad (2.6)$$

where we have integrated over a trivial overall angle, namely the azimuthal angle of the scattered lepton in the ep frame. r_L is the helicity of the incoming lepton, which is approximated to be massless, $\varepsilon = (1-y)/(1-y+y^2/2)$ is the usual ratio of longitudinal and transverse photon flux and

$$2\tilde{\Gamma} = \frac{\alpha_{em}}{\pi Q^2} \frac{1-x}{x} \left(1-y+y^2/2\right) , \quad (2.7)$$

where in the expressions of ε and $2\tilde{\Gamma}$ we have neglected terms of order $x^2 m_p^2/Q^2$. Equation (2.6) remains valid if its l.h.s. and the σ_{mn} on its r.h.s. are made differential in additional variables as described above. Since the γ^*p cross sections and interference terms are independent of φ the dependence of the ep cross section on this angle is explicitly given by the trigonometric functions in (2.6).

Let us have a closer look at those combinations of the σ_{mn} that are multiplied with the lepton helicity r_L in (2.6). To make their role more apparent we introduce differential cross sections and interference terms $d\sigma_{kl}$ with $k, l = 0, 1, 2$ analogous to the $d\sigma_{mn}$, but with the linear photon polarisations $\varepsilon_0, \varepsilon_1, \varepsilon_2$ of (2.3) instead of $\varepsilon_-, \varepsilon_0, \varepsilon_+$ in the helicity basis. We have the relations

$$\begin{aligned} \frac{1}{2}(d\sigma_{++} + d\sigma_{--}) &= \frac{1}{2}(d\sigma_{11} + d\sigma_{22}) \\ \operatorname{Re} d\sigma_{+-} &= -\frac{1}{2}(d\sigma_{11} - d\sigma_{22}) \\ \operatorname{Im} d\sigma_{+-} &= \operatorname{Re} d\sigma_{12} \\ \operatorname{Re}(d\sigma_{+0} - d\sigma_{-0}) &= -\sqrt{2} \operatorname{Re} d\sigma_{10} \\ \operatorname{Im}(d\sigma_{+0} + d\sigma_{-0}) &= \sqrt{2} \operatorname{Re} d\sigma_{20} \\ \frac{1}{2}(d\sigma_{++} - d\sigma_{--}) &= -\operatorname{Im} d\sigma_{12} \\ \operatorname{Re}(d\sigma_{+0} + d\sigma_{-0}) &= -\sqrt{2} \operatorname{Im} d\sigma_{20} \\ \operatorname{Im}(d\sigma_{+0} - d\sigma_{-0}) &= -\sqrt{2} \operatorname{Im} d\sigma_{10} . \end{aligned} \quad (2.8)$$

The terms that depend on the lepton helicity in the ep cross section are seen to be the imaginary parts of γ^*p interference terms for linearly polarised photons. $d\sigma_{kl}$ is given by $\mathcal{M}_k^* \mathcal{M}_l$ multiplied with a phase space element and real factors, summed over the appropriate final states and averaged over the initial proton spin, where we define the amplitude $e\mathcal{M}_k$ for the reaction $\gamma^*p \rightarrow X\tilde{p}$ with photon polarisation ε_k in analogy to (2.5). The imaginary parts of $d\sigma_{kl}$, $k \neq l$ are obviously zero if the phase of this amplitude does not depend on the photon polarisation. Note that any (convention dependent) phase of $|X\tilde{p} \text{ out}\rangle$ and $|p\rangle$ drops out in $d\sigma_{kl}$. Also there are no phases coming from $\varepsilon_k^*, \varepsilon_l$ because for linearly polarised photons the polarisation vectors are purely real; circular polarisation introduces extra phases in the γ^*p interference terms.

We emphasise that in order for $\text{Im } d\sigma_{kl}$ to vanish the \mathcal{M}_k do *not* have to be real. The absence of final state interactions gives vanishing interference terms if one sums over a set of final states that is invariant under time reversal (cf. [14]), but this is a sufficient condition, not a necessary one. Here we are concerned with diffraction and the phases of our amplitudes are certainly nonzero. However, for pure pomeron exchange they are given by the signature factor and thus independent of the γ^* polarisation. It is beyond the scope of this paper to investigate whether for example the superposition of pomeron exchange with exchange of secondary trajectories or with multiple exchanges could lead to polarisation dependent phases that might be tested with longitudinally polarised lepton beams.

Going back to the σ_{mn} for photons with definite helicity, we now make use of the parity invariance of strong interactions. It relates σ_{mn} for different m, n , provided that the selection criteria are parity invariant and that h is a vector, not a pseudovector. By an argument as in [9] one can show that under these conditions

$$\sigma_{mn}(W^2, Q^2) = (-1)^{m+n} \sigma_{-m, -n}(W^2, Q^2) . \quad (2.9)$$

Using this and the hermiticity of σ_{mn} one obtains the relations

$$\sigma_{++} = \sigma_{--}, \quad \sigma_{+-} = \sigma_{-+} = \sigma_{+-}^*, \quad \sigma_{+0} = -\sigma_{-0} , \quad (2.10)$$

so that the expression (2.6) of the cross section is simplified:

$$\begin{aligned} \frac{d\sigma(ep \rightarrow e\tilde{p}X)}{dx dQ^2 d\varphi} = \frac{2\tilde{\Gamma}}{2\pi} \left\{ \sigma_{++} + \varepsilon\sigma_{00} - \varepsilon \cos(2\varphi) \sigma_{+-} \right. \\ \left. - 2\sqrt{\varepsilon(1+\varepsilon)} \cos \varphi \text{Re } \sigma_{+0} + 2r_L \sqrt{\varepsilon(1-\varepsilon)} \sin \varphi \text{Im } \sigma_{+0} \right\} . \end{aligned} \quad (2.11)$$

For linear photon polarisations the relations corresponding to (2.9) read

$$\sigma_{20} = \sigma_{02} = \sigma_{21} = \sigma_{12} = 0 , \quad (2.12)$$

i.e. transverse photons with polarisation perpendicular to h_T of (2.4) do not interfere when the final state momenta are integrated over. Expressions analogous to (2.9) to (2.12) are also valid for differential γ^*p cross sections and interference terms, provided that they depend only on parity even variables, i.e. that one sums the $d\sigma_{mn}$ over a parity invariant set of final states.

2.1 Bounds on the cross section for longitudinal photons

We now show how the measurement of the φ -dependence in the ep cross section (2.11) can be used to constrain the γ^*p cross section for longitudinal photons as was pointed out in [9]. $d\sigma_{mn}$ is a positive semidefinite matrix, which with the simplifications from hermiticity and (2.9) from parity invariance implies [9]

$$\sigma_{++} + \sigma_{+-} \geq 0 , \quad \sigma_{00}(\sigma_{++} - \sigma_{+-}) \geq 2|\sigma_{+0}|^2 . \quad (2.13)$$

From the measurement of the φ -dependence in (2.11) one can extract the weighted sum $\sigma_\varepsilon = \sigma_{++} + \varepsilon\sigma_{00}$ of transverse and longitudinal γ^*p cross sections as well as the interference terms σ_{+-} , $\text{Re}\sigma_{+0}$ and $\text{Im}\sigma_{+0}$. For $\text{Im}\sigma_{+0}$ one needs longitudinally polarised electron or positron beams. With unpolarised beams one can use the weaker constraints obtained by replacing $|\sigma_{+0}|$ with $\text{Re}\sigma_{+0}$ in (2.13) and in the following.

Substituting $\sigma_\varepsilon - \varepsilon\sigma_{00}$ for σ_{++} in (2.13) the first condition gives

$$\sigma_{00} \leq \frac{\sigma_\varepsilon + \sigma_{+-}}{\varepsilon} , \quad (2.14)$$

whereas the second becomes a quadratic inequality in σ_{00} which leads to

$$\begin{aligned} \frac{\sigma_\varepsilon - \sigma_{+-}}{2\varepsilon} - \sqrt{\left(\frac{\sigma_\varepsilon - \sigma_{+-}}{2\varepsilon}\right)^2 - \frac{2|\sigma_{+0}|^2}{\varepsilon}} &\leq \sigma_{00} , \\ \sigma_{00} &\leq \frac{\sigma_\varepsilon - \sigma_{+-}}{2\varepsilon} + \sqrt{\left(\frac{\sigma_\varepsilon - \sigma_{+-}}{2\varepsilon}\right)^2 - \frac{2|\sigma_{+0}|^2}{\varepsilon}} . \end{aligned} \quad (2.15)$$

Note that the constraints in (2.15) are the better the larger $|\sigma_{+0}|$ is compared with $\sigma_\varepsilon - \sigma_{+-}$. This is what one would intuitively expect: a large interference term between longitudinal and transverse polarisations implies that neither σ_{00} nor σ_{++} can be very small, i.e. σ_{00} can be neither very small nor very large compared with σ_ε . For $|\sigma_{+0}| \ll \sigma_\varepsilon - \sigma_{+-}$ the bounds (2.15) are less stringent; they then differ only by terms of relative order $|\sigma_{+0}|^2/(\sigma_\varepsilon - \sigma_{+-})^2$ from the weaker (but simpler) conditions

$$\frac{2|\sigma_{+0}|^2}{\sigma_\varepsilon - \sigma_{+-}} \leq \sigma_{00} \leq \frac{\sigma_\varepsilon - \sigma_{+-}}{\varepsilon} . \quad (2.16)$$

By taking the derivative of (2.14) to (2.16) with respect to ε one can see that all bounds are decreasing with ε if the cross sections σ_{++} , σ_{00} and interference terms σ_{+-} , σ_{+0} are kept fixed, so that the lower bound is better for smaller ε , i.e. larger y , whereas the opposite holds for the upper bounds. Notice however that at fixed s a change in $y = (W^2 + Q^2 - m_p^2)/(s - m_p^2)$ means a change in $W^2 + Q^2$ and will also change the σ_{mn} . If their dependence on $W^2 + Q^2$ is only through a common global factor then this factor drops out in the ratios between the bounds on σ_{00} and σ_{00} itself.

Bounds of the form (2.14) to (2.16) can also be derived for differential γ^*p cross sections and interference terms if they satisfy parity constraints analogous to (2.9), i.e. if they depend only on parity invariant variables. Thus one can obtain bounds on σ_{00} by evaluating inequalities analogous to (2.14) and (2.15) for differential cross sections and then integrating them.

The usefulness of the bounds derived here depends of course on how large the interference terms are. They will in general be better in some parts of phase space than in others, a point we will illustrate in section 3.3.

An important point is that this method allows to *constrain* the longitudinal cross section for *fixed* ε , i.e. fixed y . As is well known, a *measurement* of the longitudinal cross section requires a variation of y , which means that one must either measure the ep cross section at different c.m. energies \sqrt{s} , or, if s is kept fixed, have information on how the transverse and longitudinal γ^*p cross sections depend on $W^2 + Q^2$.

We finally remark that up to now we have not used the requirement of a fast outgoing proton or a rapidity gap between X and the proton remnant \tilde{p} in reaction (2.1). The analysis developed here, and in particular the possibility to constrain the longitudinal cross section, is directly applicable to ordinary deep inelastic scattering. In fact, there has been much work on azimuthal correlations in exclusive or semi-inclusive hadron production and in semi-inclusive jet production [13], with the vector h defining the azimuthal angle φ taken as the momentum of the hadron or jet, resp. The φ -dependence of the ep cross section is always given by (2.6), (2.11) with γ^*p cross sections and interference terms σ_{mn} appropriately defined for the process and angle under consideration.

3 Azimuthal dependence of dijet production

3.1 Kinematics

Our first example of an azimuthal angle in diffraction concerns events where the proton is scattered elastically and the diffractive final state X consists of a quark-antiquark pair at parton level,

$$e(k) + p(p) \rightarrow e(k') + p(\tilde{p}) + q(P_q) + \bar{q}(P_{\bar{q}}) \quad , \quad (3.1)$$

which hadronises into two jets. We allow for a finite mass m_q of the quark and antiquark. For the vector defining a direction in the dijet system we choose

$$h = P = \frac{1}{2}(P_q - P_{\bar{q}}) \quad (3.2)$$

and work in a reference frame where the incoming p is collinear with the γ^* , the photon momentum defining the z axis, and where the total momentum of the $q\bar{q}$ -pair along this axis is zero. It is related to the γ^*p c.m. by a boost in z direction, so that azimuthal angles are the same in both frames. We introduce the azimuthal angle $\varphi_{q\bar{q}}$ between the electron momentum \mathbf{k} and \mathbf{P} as in sec. 2, and the azimuthal angle χ between \mathbf{P} and Δ , where $\Delta = p - \tilde{p}$ is the momentum transfer from the proton. We will integrate over χ in the present section. Another useful variable is the longitudinal component P_L of \mathbf{P} , and thus of \mathbf{P}_q , along the photon direction. Its range is from $-P_L^{max}$ to P_L^{max} with $P_L^{max} = \sqrt{M_X^2/4 - m_q^2}$, and thus independent of χ . This is in contrast to the length of the transverse

part \mathbf{P}_T of \mathbf{P} since

$$\mathbf{P}_T^2 = \frac{M_X^2/4 - m_q^2 - P_L^2}{1 + t/(M_X^2 - t) \cdot \cos^2 \chi} . \quad (3.3)$$

Only for $t = 0$ do the transverse momenta of q and \bar{q} balance; then \mathbf{P}_T^2 is just the squared transverse jet momentum. P_L is parity invariant, which will allow us to use the simplified expression (2.11) instead of (2.6) to obtain the $\varphi_{q\bar{q}}$ -dependence of the ep cross section.

Experimentally it is difficult to establish which of the two jets originated in the quark q and which in the antiquark \bar{q} . It is therefore useful to sum over final states where the momenta of q and \bar{q} are interchanged, in other words over P and $-P$. One can show that after this symmetrisation the transverse and longitudinal γ^*p cross sections and the transverse-transverse interference terms are even in P_L , whereas the transverse-longitudinal interference terms are odd in P_L and vanish at $P_L = 0$.

To define an azimuthal angle after summing over P and $-P$ one can distinguish the two jets kinematically, e.g. according to which one points in the forward direction with respect to the photon. Let P_F be the four-momentum of the forward and P_B that of the backward jet, and choose for the direction h instead of (3.2)

$$h = P_{FB} = \frac{1}{2}(P_F - P_B) \quad (3.4)$$

with the corresponding relative azimuthal angle φ_{FB} between \mathbf{k} and \mathbf{P}_{FB} . The longitudinal component of \mathbf{P}_{FB} is $|P_L|$. Writing $P_{FB} = \text{sgn}(P_L) \cdot P$ we see that P_{FB} is a polar vector so that we can again use (2.11) for the ep cross section.

In the case $P_L = 0$, i.e. when the jet momenta are perpendicular to the γ^*p axis, eq. (3.4) leaves the sign of h undefined, as the attribution of P_F and P_B to the jets is ambiguous. This leads to an ambiguity between azimuthal angles φ_{FB} and $\varphi_{FB} + \pi$ and hence a sign ambiguity for $\cos \varphi_{FB}$ and $\sin \varphi_{FB}$ but not for $\cos(2\varphi_{FB})$ and $\sin(2\varphi_{FB})$. As mentioned above the transverse-longitudinal interference terms vanish at $P_L = 0$ when summed over P and $-P$, so that no ambiguity remains in the ep cross section.

The summation over P and $-P$ is in fact trivial under the assumption that the diffractive exchange has definite charge conjugation parity, which is of course the case for pomeron or two-gluon exchange. Applying charge conjugation invariance of the strong interactions to the photon dissociation part of the γ^*p subreaction it then follows that the differential cross section for (3.1) remains the same if we exchange q and \bar{q} :

$$d\sigma(ep \rightarrow ep + q(P_q) + \bar{q}(P_{\bar{q}})) = d\sigma(ep \rightarrow ep + \bar{q}(P_q) + q(P_{\bar{q}})) . \quad (3.5)$$

To sum over P and $-P$ and change from the variable P to P_{FB} we thus only need to multiply the cross section with 2 and replace $\varphi_{q\bar{q}}$ with φ_{FB} and P_L with $|P_L|$.

3.2 The dijet cross section at $t = 0$ in the Landshoff-Nachtmann model

In this subsection we give the differential cross section for reaction (3.1) at $t = 0$ in the model of Landshoff and Nachtmann (LN) [12, 16]. The transverse and longitudinal γ^*p cross sections have been computed in [6], and the calculation of the interference terms goes along the same lines. We therefore only recall the essentials of the model and give the final results.

The LN model was developed to give a simple QCD based description of the soft pomeron. It approximates pomeron exchange by the exchange of two gluons which are taken as nonperturbative, i.e. they have a nonperturbative propagator $-g_{\mu\nu}D(l^2)$ instead of $-g_{\mu\nu}/l^2$ in Feynman gauge. The nonperturbative propagator $D(l^2)$ is a difficult quantity to compute and indeed there is no consensus in the literature about its behaviour at small l^2 [17], but we will not attempt to discuss this issue here. We will instead follow the rather model independent approach of [12, 16, 18], which is based on the observation that often the amplitude of a considered process can be approximated in such a way that it depends on $D(l^2)$ only via certain simple integrals, so that it is not necessary to know the detailed functional form of $D(l^2)$. In the present paper we will need the two moments

$$\int_0^\infty dl^2 [\alpha_s^{(0)} D(-l^2)]^2 = \frac{9\beta_0^2}{4\pi} , \quad (3.6)$$

$$\int_0^\infty dl^2 [\alpha_s^{(0)} D(-l^2)]^2 \cdot l^2 = \frac{9\beta_0^2 \mu_0^2}{8\pi} , \quad (3.7)$$

where $\beta_0 \approx 2.0 \text{ GeV}^{-1}$ and $\mu_0 \approx 1.1 \text{ GeV}$ have been estimated from data [16, 18]. From the ratio of (3.7) and (3.6) μ_0^2 appears as the scale characteristic for the behaviour of D on l^2 . Following [18] we take $\alpha_s^{(0)} \approx 1$ for the strong coupling in the nonperturbative region which dominates the l^2 -integrations in (3.6), (3.7).

In this model the reaction $\gamma^*p \rightarrow q\bar{q}p$ is described by the exchange of two gluons between a quark in the proton and the $q\bar{q}$ -pair into which the virtual photon splits. In the high-energy limit its amplitude is purely imaginary and thus can be calculated by cutting the corresponding Feynman diagrams in the s -channel. In each diagram there is then exactly one off-shell quark, namely one of the quarks into which the photon dissociates. Its typical virtuality is

$$\lambda^2 = \frac{\mathbf{P}_T^2 + m_q^2}{1 - \beta} = (M_X^2 + Q^2) \frac{\mathbf{P}_T^2 + m_q^2}{M_X^2} , \quad (3.8)$$

which can be seen as the relevant scale of hardness of the process [4, 19]. We obtain the ep cross section from the master equation (2.11) as

$$\begin{aligned} \frac{d\sigma(ep \rightarrow ep q\bar{q})}{d\varphi_{q\bar{q}} dx dQ^2 dP_L d\beta dt} &= \frac{\alpha_{em}}{\pi} \frac{1}{2\pi x Q^2} (1 - y + y^2/2) \left\{ \frac{d\sigma_{++}^{q\bar{q}}}{dP_L d\beta dt} + \varepsilon \frac{d\sigma_{00}^{q\bar{q}}}{dP_L d\beta dt} \right. \\ &\quad \left. - \varepsilon \cos(2\varphi_{q\bar{q}}) \frac{d\sigma_{+-}^{q\bar{q}}}{dP_L d\beta dt} - 2\sqrt{\varepsilon(1+\varepsilon)} \cos \varphi_{q\bar{q}} \frac{d\sigma_{+0}^{q\bar{q}}}{dP_L d\beta dt} \right\} . \end{aligned} \quad (3.9)$$

$d\sigma_{+0}^{q\bar{q}}/(dP_L d\beta dt)$ is purely real in our approximation since the γ^*p amplitude is purely imaginary, so that its phase is independent of the photon polarisations, see our discussion in sec. 2. For the differential γ^*p cross sections and interference terms we find

$$\left. \frac{d\sigma_{mn}^{q\bar{q}}}{dP_L d\beta dt} \right|_{t=0} = \frac{8}{3} \alpha_{em} e_q^2 \frac{\alpha_s(\lambda^2)}{\alpha_s^{(0)}} \xi^{2(1-\alpha_P(0))} \frac{1-\beta}{\beta M_X (M_X^2 + Q^2)^2} \mathcal{S}_{mn}^{q\bar{q}} , \quad (3.10)$$

where e_q is the electric charge of the produced quark in units of the positron charge and $\alpha_P(t) = 1 + \epsilon + \alpha' t$ with $\epsilon \approx 0.085$ and $\alpha' \approx 0.25 \text{ GeV}^{-2}$ the soft pomeron trajectory. The reduced cross sections

$$\begin{aligned} \mathcal{S}_{++}^{q\bar{q}} &= \left(1 - 2 \frac{\mathbf{P}_T^2 + m_q^2}{M_X^2} \right) \frac{\mathbf{P}_T^2}{\mathbf{P}_T^2 + m_q^2} (M_X^2 + Q^2)^2 L_1(\mathbf{P}_T^2, w)^2 \\ &\quad + \frac{m_q^2}{\mathbf{P}_T^2 + m_q^2} (M_X^2 + Q^2)^2 L_2(\mathbf{P}_T^2, w)^2 , \\ \mathcal{S}_{00}^{q\bar{q}} &= 4 \frac{Q^2}{M_X^2} \frac{\mathbf{P}_T^2 + m_q^2}{M_X^2} (M_X^2 + Q^2)^2 L_2(\mathbf{P}_T^2, w)^2 , \\ \mathcal{S}_{+-}^{q\bar{q}} &= 2 \frac{\mathbf{P}_T^2 + m_q^2}{M_X^2} \frac{\mathbf{P}_T^2}{\mathbf{P}_T^2 + m_q^2} (M_X^2 + Q^2)^2 L_1(\mathbf{P}_T^2, w)^2 , \\ \mathcal{S}_{+0}^{q\bar{q}} &= -2\sqrt{2} \frac{Q}{M_X} \frac{P_L |\mathbf{P}_T|}{M_X^2} (M_X^2 + Q^2)^2 L_1(\mathbf{P}_T^2, w) L_2(\mathbf{P}_T^2, w) , \end{aligned} \quad (3.11)$$

whose normalisation has been chosen for later convenience, involve loop integrals

$$L_i(\mathbf{P}_T^2, w) = \int_0^\infty d\mathbf{l}_T^2 [\alpha_s^{(0)} D(-\mathbf{l}_T^2)]^2 f_i(v, w) , \quad i = 1, 2 \quad (3.12)$$

over the functions

$$\begin{aligned} f_1(v, w) &= 1 - \frac{1}{2w} \left[1 - \frac{v+1-2w}{\sqrt{(v+1-2w)^2 + 4w(1-w)}} \right] , \\ f_2(v, w) &= 1 - \frac{1}{\sqrt{(v+1-2w)^2 + 4w(1-w)}} \end{aligned} \quad (3.13)$$

of the dimensionless variables³

$$v = \frac{\mathbf{l}_T^2}{\lambda^2} , \quad w = \frac{\mathbf{P}_T^2}{\lambda^2} = (1-\beta) \frac{\mathbf{P}_T^2}{\mathbf{P}_T^2 + m_q^2} . \quad (3.14)$$

Assuming that due to the squared gluon propagator the dominant values of \mathbf{l}_T^2 in the loop integrals L_i are small compared with λ^2 we can Taylor expand $f_i(v, w)$ at $v = 0$ and approximate

$$f_i(v, w) \approx v \cdot \left. \frac{\partial f_i(v, w)}{\partial v} \right|_{v=0} , \quad (3.15)$$

³The definitions of v and w here differ from those in [6].

so that the remaining integral is given by (3.7). The integral (3.6) does not appear because both f_1 and f_2 vanish at $v = 0$. In this approximation (3.11) becomes

$$\begin{aligned}
\mathcal{S}_{++}^{q\bar{q}} &= \left(\frac{9\beta_0^2 \mu_0^2}{8\pi} \right)^2 \left\{ 4 \left(\frac{M_X^2}{\mathbf{P}_T^2 + m_q^2} \right)^2 \left(1 - 2 \frac{\mathbf{P}_T^2 + m_q^2}{M_X^2} \right) \frac{\mathbf{P}_T^2}{\mathbf{P}_T^2 + m_q^2} (1-w)^2 \right. \\
&\quad \left. + \left(\frac{M_X^2}{\mathbf{P}_T^2 + m_q^2} \right)^2 \frac{m_q^2}{\mathbf{P}_T^2 + m_q^2} (1-2w)^2 \right\} , \\
\mathcal{S}_{00}^{q\bar{q}} &= \left(\frac{9\beta_0^2 \mu_0^2}{8\pi} \right)^2 \cdot 4 \frac{Q^2}{M_X^2} \cdot \frac{M_X^2}{\mathbf{P}_T^2 + m_q^2} (1-2w)^2 , \\
\mathcal{S}_{+-}^{q\bar{q}} &= \left(\frac{9\beta_0^2 \mu_0^2}{8\pi} \right)^2 \cdot 8 \frac{M_X^2}{\mathbf{P}_T^2 + m_q^2} \cdot \frac{\mathbf{P}_T^2}{\mathbf{P}_T^2 + m_q^2} (1-w)^2 , \\
\mathcal{S}_{+0}^{q\bar{q}} &= - \left(\frac{9\beta_0^2 \mu_0^2}{8\pi} \right)^2 \cdot 4\sqrt{2} \frac{Q}{M_X} \cdot \frac{M_X^2}{\mathbf{P}_T^2 + m_q^2} \frac{P_L |\mathbf{P}_T|}{\mathbf{P}_T^2 + m_q^2} (1-w)(1-2w) .
\end{aligned} \tag{3.16}$$

As a benchmark we have compared the integrals $L_i(\mathbf{P}_T^2, w)$ in the approximation (3.15) with their exact values for the model gluon propagator used in [16]:

$$D(-l^2) \propto \left[1 + \frac{l^2}{(n-1)\mu_0^2} \right]^{-n} , \quad n \geq 4 , \tag{3.17}$$

where the proportionality constant can easily be obtained from (3.6). For $n \rightarrow \infty$ this becomes $D(-l^2) \propto \exp(-l^2/\mu_0^2)$. We find that the value of n has little influence on the $L_i(\mathbf{P}_T^2, w)$, and that the approximations (3.15) are in general rather good, except however for some regions of parameter space. In particular the approximation of L_1 becomes bad for w close to 1 and for small \mathbf{P}_T^2 . On the other hand L_2 becomes zero and changes its sign for some \mathbf{P}_T^2 if $w > 1/2$ because the function $f_2(v)$ changes sign at $v = w \cdot \mathbf{l}_T^2 / \mathbf{P}_T^2 = 2(2w-1)$. The parameters \mathbf{P}_T^2, w for which L_2 vanishes are not always well reproduced by the approximation; it can be seen that for given \mathbf{P}_T^2 the value $w = 1/2$ obtained from (3.15) is too small, so that with fixed m_q^2 the corresponding value of β is overestimated

An improved approximation, also leading to the moment (3.7), is achieved by replacing (3.15) with

$$f_i(v, w) \approx v \cdot \frac{f_i(v_0, w)}{v_0} , \quad v_0 = \frac{l_0^2}{\lambda^2} , \tag{3.18}$$

where we take $l_0^2 = \mu_0^2$. With this approximation the values \mathbf{P}_T^2, w where L_2 vanishes are reproduced much better, and the errors on L_1 are in the region of a few percent even if $w = 0.9$ and \mathbf{P}_T^2 as small as 2 GeV².

3.3 Discussion of the results

Let us make some remarks on the results (3.11), (3.16). The first concerns the sign of the γ^*p interference terms. The transverse-transverse interference is always positive, so that the term with $\cos(2\varphi_{q\bar{q}})$ in the ep cross section (3.9) is negative. In [11] it was pointed out that this is the opposite sign than the one obtained for $q\bar{q}$ -production in photon-gluon fusion. The sign of the longitudinal-transverse interference depends on the loop integral $L_2(\mathbf{P}_T^2, w)$ and thus on the value of w . (3.16) gives a sign change at $w = 1/2$, the exact value of w from (3.11) is larger and depends on \mathbf{P}_T^2 as mentioned at the end of the previous subsection. This characteristic change of sign has also been observed in [11]. As a general remark we can say that the distribution of the ep cross section in $\varphi_{q\bar{q}}$ we obtain is very similar to the one in the perturbative two-gluon approach of [11], apart from the overall normalisation which comes out different in the two models, cf. [20]. The main characteristics of the normalised azimuthal distribution are determined by the two-gluon exchange picture.

We now turn to the dependence on the transverse jet momentum. From (3.11) one sees that compared with the transverse cross section the transverse-longitudinal interference is suppressed by a factor $|\mathbf{P}_T|/M_X$, the transverse-transverse interference by \mathbf{P}_T^2/M_X^2 and the longitudinal cross section by $(\mathbf{P}_T^2 + m_q^2)/M_X^2$. This means that the interferences (and the longitudinal cross section) are less important if \mathbf{P}_T^2 is small compared with M_X^2 , i.e. if the jets are close to the γ^*p axis in the reference frame we are working in. Note that for light quarks the suppression of the transverse-longitudinal interference is weaker than the one for the longitudinal cross section. This suggests a way to experimentally look for the zero in the longitudinal γ^*p amplitude, which is due to the behaviour of the integral $L_2(\mathbf{P}_T^2, w)$ and can be viewed as a characteristic feature of the two-gluon exchange mechanism in this reaction: The zero might be seen through the change of sign of the $\cos \varphi_{q\bar{q}}$ -term in the angular dependence as w or β is varied, whereas it should be difficult to observe it from a dip in the $\varphi_{q\bar{q}}$ -integrated spectra, given that the longitudinal γ^*p cross section is much smaller than the transverse one where the zero occurs. We finally note that for heavy quarks (3.11) is valid down to $\mathbf{P}_T^2 = 0$ and that all interference terms (though not the longitudinal cross section) vanish in this limit where h is collinear with p and q as required by angular momentum conservation.

For a numerical study we change variables from $\varphi_{q\bar{q}}$ and P_L to φ_{FB} and $|P_L|$ as explained at the end of sec. 3.1 and integrate over $|P_L|$. To ensure that we have jets and that the scale λ^2 of (3.8) remains large we impose a lower cut \mathbf{P}_{Tcut}^2 on \mathbf{P}_T^2 , which at $t = 0$ corresponds to an m_q^2 -dependent upper cut P_{Lcut} on $|P_L|$, see (3.3). The φ_{FB} -dependence of the ep cross section for the quark flavours u, d, s, c at the HERA c.m. energy of $\sqrt{s} = 296$ GeV is shown in fig. 1, where we plot $d\sigma(ep \rightarrow ep q\bar{q})/(d\varphi_{FB} dx dQ^2 d\beta dt)$ as a function of φ_{FB} for different values of the other kinematical variables. We note that in the examples where charmed

jets can be produced kinematically their fraction in the γ^*p cross section is not negligible; for cases (a) and (b) of the table in fig. 1 it is about 1/3, and for case (e) about 1/5.

The examples in fig. 1 illustrate how a smaller minimum \mathbf{P}_T^2/M_X^2 leads to a flatter dependence on φ_{FB} as discussed above, while increasing the overall rate. The effect of β on the sign of the $\cos \varphi_{FB}$ -term in the cross section can clearly be seen. Also shown in the plots is the difference between the approximations (3.18) and (3.15) of the integrals in (3.11): in general the less exact approximation (3.15) which leads to (3.16) is rather good, especially if \mathbf{P}_{Tcut}^2 is large.

Finally we investigate what bounds on the longitudinal γ^*p cross section one could obtain from measuring the φ_{FB} -dependence shown in fig. 1. For convenience we introduce the quantities

$$\begin{aligned} F_{++}^{FB} &= \frac{d\sigma_{++}^{FB}}{d\beta dt}, & F_{00}^{FB} &= \varepsilon \frac{d\sigma_{00}^{FB}}{d\beta dt}, & F_{\varepsilon}^{FB} &= F_{++}^{FB} + F_{00}^{FB}, \\ F_{+-}^{FB} &= -\varepsilon \frac{d\sigma_{+-}^{FB}}{d\beta dt}, & F_{+0}^{FB} &= -2\sqrt{\varepsilon(1+\varepsilon)} \frac{d\sigma_{+0}^{FB}}{d\beta dt}, \end{aligned} \quad (3.19)$$

whose factors are chosen such that

$$\begin{aligned} \frac{d\sigma(ep \rightarrow ep q\bar{q})}{d\varphi_{FB} dx dQ^2 d\beta dt} &= \frac{\alpha_{em}}{\pi} \frac{1}{2\pi x Q^2} (1 - y + y^2/2) \\ &\quad \left\{ F_{\varepsilon}^{FB} + F_{+-}^{FB} \cos(2\varphi_{FB}) + F_{+0}^{FB} \cos \varphi_{FB} \right\}. \end{aligned} \quad (3.20)$$

Up to a global factor F_{ε}^{FB} , F_{+0}^{FB} and F_{+-}^{FB} are therefore the Fourier coefficients for the φ_{FB} -dependence of the ep cross section, and F_{00}^{FB} is the contribution of longitudinal photons to F_{ε}^{FB} . Table 1 gives the coefficients F_{+-}^{FB} , F_{+0}^{FB} and F_{ε}^{FB} which correspond to the plots in fig. 1, the longitudinal contributions F_{00}^{FB} , and the lower and upper bounds F_{low}^{FB} , F_{upp}^{FB} on F_{00}^{FB} one can obtain from the φ_{FB} -dependence using the differential analogues of (2.15). The upper bound (2.14) is not useful since the transverse-transverse interference $d\sigma_{+-}^{FB}/(d\beta dt)$ is positive.

When the minimum \mathbf{P}_T^2/M_X^2 is rather small, i.e. in cases (b) and (e), the lower and upper bounds are rather far apart from each other and in this sense not very stringent, due to the suppression of the transverse-longitudinal interference by $|\mathbf{P}_T|/M_X$ compared with the transverse cross section. From (2.16) we see that the lower bound is then suppressed by \mathbf{P}_T^2/M_X^2 . On the other hand the longitudinal cross section itself has a suppression factor $(\mathbf{P}_T^2 + m_q^2)/M_X^2$, and as a result the lower bound we obtain is quite close to the actual value of F_{00}^{FB} .

3.4 Jet angle for more general final states

We now generalise the jet angle used so far to diffractive final states X that do not necessarily have a two-jet topology. As before we work in a reference frame where the incoming photon and proton are collinear and where the total momentum of

Table 1: Fourier coefficients corresponding to the angular distributions shown in fig. 1 and lower and upper bounds F_{low}^{FB} , F_{upp}^{FB} on the longitudinal contribution F_{00}^{FB} one can obtain from them. For the definition of F_{ε}^{FB} , F_{00}^{FB} etc. cf. (3.19). $y = 0.5$, $\varepsilon = 0.8$, $\sqrt{s} = 296$ GeV, $t = 0$.

	β	M_X^2 GeV ²	\mathbf{P}_{Tcut}^2 GeV ²	F_{+-}^{FB}	F_{+0}^{FB}	F_{ε}^{FB} nb/GeV ²	F_{00}^{FB}	F_{low}^{FB}	F_{upp}^{FB}
(a)	1/3	80	16	-2.9	-0.75	4.6	0.45	0.22	0.72
(b)	1/3	80	4	-11	-7.1	43	1.3	0.50	28
(c)	2/3	20	4	-8.3	3.5	15	2.6	1.0	3.3
(d)	1/3	20	4	-54	-14	86	7.2	4.1	14
(e)	2/3	20	1	-30	49	130	18	8.4	80

X along this axis is zero. Let $\boldsymbol{\tau}$ be the thrust axis of X in this frame. It can be oriented by requiring that it points in the direction of the photon momentum:

$$\boldsymbol{\tau} = \tau \operatorname{sgn}(\mathbf{q} \cdot \boldsymbol{\tau}) . \quad (3.21)$$

This provides a direction in the hadronic final state, which we can also write as a four-vector:

$$h = (0, \boldsymbol{\tau}) . \quad (3.22)$$

From (3.21) and (3.22) it follows that h is a polar vector. Note that in the case of a two-jet final state and in the limit $t = 0$ it becomes proportional to the vector P_{FB} defined in (3.4). Another possibility would be to define h from the thrust axis in the rest frame of X by equations analogous to (3.21) and (3.22), and then to boost h to the γ^*p frame. If X is a dijet this is then proportional to P_{FB} even at finite t .

The vector h defined in one of these ways, or a vector obtained from another suitable shape variable of the system X , can be used for the definition of the azimuthal angle φ and of γ^*p cross sections and interference terms. It is not restricted to events with only two jets in X , and it does not require to have jets with a transverse momentum large enough for a jet algorithm to be applicable. This could allow for a significant gain in statistics. The measurement of the φ -dependence could in particular be used to constrain the cross section for longitudinal photons. The discussion in the previous subsection and the numerical example with $\mathbf{P}_T^2 \geq 1$ GeV² in table 1 indicates that one might obtain at least a useful lower bound even for low \mathbf{P}_T^2 , provided the ratio \mathbf{P}_T^2/M_X^2 is not very small. Too small values of \mathbf{P}_T^2/M_X^2 will presumably also present experimental problems, since then the polar angle of \mathbf{h} is close to zero and the resolution on its azimuth will become poor.

When the thrust axis is perpendicular to the γ^*p direction the requirement (3.21) does not fix its orientation, so that the angle φ is only defined up to an ambiguity between φ and $\varphi + \pi$. This is just as in the case $P_L = 0$ for the two-jet final state which was discussed at the end of sec. 3.1. Using a similar argument as there one can show that the transverse-longitudinal interference terms vanish when the thrust axis is perpendicular to \mathbf{q} so that no ambiguity appears in the ep cross section.

4 Dijet production at finite t

4.1 Coupling of the two gluons to the proton

We will now investigate diffractive production of a jet pair (3.1) at finite t in the LN model. Throughout our calculation we take the high energy limit, dropping terms that are suppressed by factors of ξ . In this approximation $t = \Delta_T^2$ where Δ_T is the transverse part of Δ with respect to p and q . A characteristic property of the LN model is that the two gluons couple to the same quark in a hadron [12]. The coupling of the gluons to the proton is then given by the isoscalar vector current of the nucleon, and the squared amplitude for the process is proportional to [9]

$$\tilde{G}^2(t) = F_1^2(t) - \frac{t}{4m_p^2} F_2^2(t) . \quad (4.1)$$

where $F_1(t)$ and $F_2(t)$ are the isoscalar Dirac and Pauli form factors of the nucleon, respectively, i.e. the sum of the Dirac (Pauli) form factors of the proton and the neutron. At $t = 0$ one has $F_1(0) = 1$ and $F_2(0) \approx -0.12$, cf. [9], and in the region $|t| \lesssim 1 \text{ GeV}^2$ we are interested in $F_1(t)$ is dominating this expression.

One finds that at high energy the relevant kinematics in the Feynman diagrams for $\gamma^*p \rightarrow q\bar{q}p$ are determined by the proton momentum and the kinematic variables of the $\gamma^* \rightarrow q\bar{q}$ transition, but not on the momentum of the quark within the proton. All dependence of the amplitude on the nucleon structure thus comes from the form factor $\tilde{G}(t)$; there is no further dependence on transverse or longitudinal momentum distributions of quarks, even at finite Δ_T .

The polarisation vectors for the gluons coupling to the proton both come out proportional to the initial proton momentum p . For the complete amplitude they are contracted with the propagators of the gluons, and the result is contracted with a tensor corresponding to the gluons coupling to the produced quark and antiquark. We wish to remark that one need not take a Feynman-like gauge for the gluons, i.e. a propagator $-g_{\mu\nu}D(k^2)$ where k is the gluon momentum. In fact one has some freedom to choose a gauge in our model without changing the structure of the result: there is no contribution to the amplitude from the tensor $k_\mu k_\nu$ in a general covariant gauge, nor from $k_\mu n_\nu + n_\mu k_\nu$ with some fixed four-vector n , which appears in non-covariant gauges. The reason is that in the

approximation of our calculation the exchanged gluons couple directly to quarks, not to gluons, and thus to a conserved vector current. Note however that for terms in the propagator which involve $n_\mu n_\nu$ (appearing in radiative corrections to the bare propagator in non-covariant gauges) one would have to investigate in detail whether the extra tensors contribute to the leading energy behaviour of the amplitude.

The approximation of two noninteracting gluons in the LN model is certainly a very crude one. To go beyond it one could replace the direct coupling of the gluons to a quark in the proton by the cut amplitude for the emission by the proton of two gluons, in other words by the cut amplitude for $g^*p \rightarrow g^*p$. Including the gluon propagators the latter might be approximated by the gluon distribution in the proton [21, 4] at zero t . This is however not useful when we want to compute the effects of finite t , since in the gluon distribution the four-momenta of the two gluons are by definition equal, in particular they do not transfer any transverse momentum Δ_T .

Some features of the LN model are also found in this more general framework if one makes the assumption that the squared c.m. energy of the $g^*p \rightarrow g^*p$ amplitude is small compared to W^2 in the region of phase space which dominates the amplitude for $\gamma^*p \rightarrow q\bar{q}p$. This is for instance the case in the multiperipheral approximation. Then one can show that the polarisation of the gluons is again proportional to p , and that the relevant kinematics in the Feynman diagrams are as in the LN model calculation. Moreover, both statements remain valid if the proton dissociates and one integrates over the particle momenta in the proton remnant with \tilde{p} being held fixed, provided that $\tilde{p}^2 \ll W^2$.

What is however particular to our model is the dependence of the amplitude for the emission of two gluons by the proton and their propagation on t and, yet more importantly, on the gluon virtualities, the latter being given by the nonperturbative gluon propagators. We shall see that precisely these two points will have the main effect on the t -dependence of the cross section for our process.

4.2 Loop integration

Having contracted the tensor for the two gluons coupling to the proton with the one for their coupling to the $\gamma^* \rightarrow q\bar{q}$ transition we must perform a loop integration. We label the loop momentum l in such a way that the first gluon emitted from the proton carries momentum $-l + \Delta/2$ and the second gluon $l + \Delta/2$. Their respective virtualities come out as $(l - \Delta/2)^2 = (l_T - \Delta_T)^2$ and $(l + \Delta/2)^2 = (l_T + \Delta_T)^2$, where l_T is the transverse part of l with respect to p and q . Using the cutting rules we are left with a two-dimensional loop integral of the form

$$L[f] = \int \frac{d^2 l_T}{\pi} [\alpha_s^{(0)}]^2 D \left[-(\mathbf{l}_T - \mathbf{\Delta}_T/2)^2 \right] D \left[-(\mathbf{l}_T + \mathbf{\Delta}_T/2)^2 \right] \cdot f \quad (4.2)$$

with some complicated function f depending on \mathbf{l}_T , Δ_T and the other kinematical variables \mathbf{P}_T , m_q , M_X , Q^2 . In particular f contains quark propagators whose denominators depend on $\mathbf{l}_T \cdot \Delta_T$ and $\mathbf{l}_T \cdot \mathbf{P}_T$ so that unlike in the case $t = 0$ we cannot now perform the integration over the angle of \mathbf{l}_T without specifying a model for the gluon propagator D . To obtain a more transparent representation of the model dependence and to avoid numerical integrations already at amplitude level we expand those quark propagators up to second order in $(\mathbf{l}_T - \Delta_T/2)$, assuming that both $|\mathbf{l}_T|$ and $|\Delta_T|$ are sufficiently small. The expansion requires

$$\mathbf{l}_T^2 \ll \lambda^2, \quad |\mathbf{l}_T \cdot \mathbf{P}_T| \ll \lambda^2, \quad \Delta_T^2 \ll \lambda^2, \quad (4.3)$$

where

$$\lambda^2 = \frac{M_X^2/4 - t/4 - P_L^2}{1 - \beta} \quad (4.4)$$

is a generalisation to finite t of the scale (3.8). Note that the first condition is what we used in the approximation (3.15) in sec. 3.2, which was a Taylor expansion around $\mathbf{l}_T^2/\lambda^2 = 0$. Our calculation will not give an expression analogous to (3.11) that does not require the gluon virtuality to be small compared with the virtuality of the off-shell quark.

To obtain tractable expressions we also expand denominators in those terms which depend on the angle χ between \mathbf{P}_T and Δ_T . The cross section is then a polynomial in $\cos \chi$ and $\sin \chi$ and can easily be integrated over χ . The small parameter for these expansions is again $|\Delta_T|$, more precisely they are valid if

$$|\Delta_T \cdot \mathbf{P}_T| \ll m_q^2 + \mathbf{P}_T^2 + \Delta_T^2/4. \quad (4.5)$$

4.3 Integrals over the gluon propagators at finite t

After the expansions just described we are left with a limited number of simple loop integrals. They have the form of $L[f]$ in (4.2) with $f = 1$, l_T^i , $l_T^i l_T^j$, where $i, j = 1, 2$. The corresponding integrands depend only on \mathbf{l}_T and Δ_T so that the integrals are just functions of t . They will turn out to be crucial quantities in the discussion of our results in sections 4.4 and 5.2.

The integral with $f = l_T^i$ is zero because its integrand is odd in l_T , whereas the tensor integral with $f = l_T^i l_T^j$ is related by rotation invariance to integrals over the scalars $f = \mathbf{l}_T^2$ and $f = (\mathbf{l}_T \cdot \Delta_T)^2$. We therefore have three linearly independent integrals to evaluate and choose the combinations

$$\begin{aligned} I_0(t) &= L[1], \\ I_1(t) &= L[\mathbf{l}_T^2], \\ I_2(t) &= L[2(\mathbf{l}_T \cdot \Delta_T)^2/\Delta_T^2 - \mathbf{l}_T^2] = L[\mathbf{l}_T^2 \cos(2\delta)], \end{aligned} \quad (4.6)$$

where δ is the angle between \mathbf{l}_T and Δ_T . At $t = 0$ we have $I_0(0) = 9\beta_0^2/(4\pi)$ and $I_1(0) = 9\beta_0^2\mu_0^2/(8\pi)$ from (3.6), (3.7), while the integration over δ gives $I_2(0) = 0$.

The ratio of $I_1(0)$ and $I_0(0)$ involves the scale $\mu_0^2 \approx 1.2 \text{ GeV}^2$, which is also the characteristic scale for the t -dependence of the integrals in (4.6) since it is the typical scale for the momentum dependence of $D(l^2)$. We will therefore have two kinds of corrections to the cross sections and interference terms at zero t :

1. corrections in powers of $|t|$ divided by some kinematical variable of the γ^*p reaction, such as Q^2 , M_X^2 , or λ^2 of (4.4). By assumption these kinematical variables are all large compared with $|t|$, cf. (4.3).
2. corrections which depend on t via t/μ_0^2 , where μ_0^2 comes from the ratio of the integrals in (4.6) or from their variation with t . It is important that μ_0^2 is *not large* compared to typical values of $|t| \lesssim 1 \text{ GeV}^2$.

We have calculated the γ^*p cross sections and interference terms keeping the corrections in point 1 up to order t/Q^2 , whereas no expansion was made in t/μ_0^2 , having in mind that we can have $t/\mu_0^2 = O(1)$.

One can make a more detailed statement about the small- t behaviour of the integrals (4.6) under the assumption that the function $D(l^2)$ is sufficiently well behaved to be Taylor expanded. In (4.2) we then can expand $(\mathbf{l}_T \mp \mathbf{\Delta}_T)^2$ in the gluon propagators around \mathbf{l}_T^2 . Terms in this expansion that are odd in $\mathbf{l}_T \cdot \mathbf{\Delta}_T$ vanish after integration over the angle δ , so that the integrals have a power expansion in $\mathbf{\Delta}_T^2 = |t|$:

$$\begin{aligned}
I_0(t) &= \frac{9\beta_0^2}{4\pi} \left(1 + c_0^{(1)} \frac{|t|}{\mu_0^2} + c_0^{(2)} \left(\frac{|t|}{\mu_0^2} \right)^2 + \dots \right), \\
I_1(t) &= \frac{9\beta_0^2}{4\pi} \frac{\mu_0^2}{2} \left(1 + c_1^{(1)} \frac{|t|}{\mu_0^2} + c_1^{(2)} \left(\frac{|t|}{\mu_0^2} \right)^2 + \dots \right), \\
I_2(t) &= \frac{9\beta_0^2}{4\pi} |t| c_2^{(0)} \left(1 + c_2^{(1)} \frac{|t|}{\mu_0^2} + \dots \right). \tag{4.7}
\end{aligned}$$

On one hand (4.7) shows that the deviation of these integrals from their values at $t = 0$ is proportional to t and not to $\sqrt{-t}$. Moreover one may get a reasonable description of their t -dependence over a wider range keeping a few terms of this expansion.

We have evaluated the integrals $I_0(t)$, $I_1(t)$, $I_2(t)$ with the model (3.17) of the gluon propagator. For $n = 4$ we obtain good quadratic fits of the integrals in the range $|t| = 0$ to 1.4 GeV^2 with

$$\begin{aligned}
c_0^{(1)} &= -0.5, & c_0^{(2)} &= 0.12, & c_1^{(1)} &= -0.38, & c_1^{(2)} &= 0.09, \\
c_2^{(0)} &= 0.027, & c_2^{(1)} &= -0.31
\end{aligned} \tag{4.8}$$

and all other coefficients being zero. For $n = \infty$ we have an exponential propagator $D(-\mathbf{l}_T^2) \propto \exp\{-\mathbf{l}_T^2/\mu_0^2\}$ and easily find $I_i(t) = \exp\{-|t|/(2\mu_0^2)\} \cdot I_i(0)$ for

$i = 0, 1, 2$. Comparing the integrals for $n = 4$ and $n = \infty$ we find that they are almost equal for I_0 and that I_1 is smaller for $n = \infty$ than for $n = 4$, the coefficient $c_1^{(1)}$ for $n = \infty$ being -0.5 instead of -0.38 . I_2 vanishes at all t for the exponential propagator, for $n = 4$ it is still very small compared with $|t| \cdot I_0$.

4.4 Results

We now present our results for the γ^*p cross sections and interference terms of quark-antiquark production at finite t , the ep cross section is obtained from eq. (3.9). We first give analytical expressions including the corrections in t/μ_0^2 , but without the corrections of order t/Q^2 which are rather lengthy. The latter will be included in the numerical discussion below.

To zeroth order in t/Q^2 only two linear combinations of the integrals (4.6) appear, namely

$$K_1(t) = I_1(t) - |t| I_0(t)/4 , \quad K_2(t) = I_2(t) - |t| I_0(t)/4 . \quad (4.9)$$

From (4.7) we see that the leading term in the expansion of $K_1(t)$ in t/μ_0^2 is constant, whereas the leading term for K_2 is proportional to t/μ_0^2 . We introduce the abbreviations

$$\begin{aligned} a &= \frac{M_X^2/4 - t/4 - P_L^2}{M_X^2 - t} \xrightarrow{t \rightarrow 0} \frac{\mathbf{P}_T^2 + m_q^2}{M_X^2} , \\ b &= \frac{M_X^2/4 - m_q^2 - P_L^2}{M_X^2/4 - t/4 - P_L^2} \xrightarrow{t \rightarrow 0} \frac{\mathbf{P}_T^2}{\mathbf{P}_T^2 + m_q^2} , \end{aligned} \quad (4.10)$$

whose limits for $t \rightarrow 0$ are given for easy comparison with our results in sec. 3.2, and the variable $w = (1 - \beta) b$ as a generalisation to finite t of w defined in (3.14). The result then reads

$$\begin{aligned} \frac{d\sigma_{mn}^{q\bar{q}}}{dP_L d\beta dt} = & \frac{8}{3} \alpha_{em} e_q^2 \frac{\alpha_s(\lambda^2)}{\alpha_s^{(0)}} \tilde{G}^2(t) \xi^{2(1-\alpha_P(t))} \frac{1 - \beta}{\beta \sqrt{M_X^2 - t(M_X^2 + Q^2 - t)^2}} \mathcal{S}_{mn}^{q\bar{q}} \quad (4.11) \end{aligned}$$

with

$$\begin{aligned} \mathcal{S}_{++}^{q\bar{q}} &= \frac{K_1^2}{a^2} \left[4(1 - 2a) b (1 - w)^2 + (1 - b)(1 - 2w)^2 \right] + \\ &\quad \frac{K_2^2}{a^2} \left[(1 - 2a) b (1 - 2w + 2w^2) + 2(1 - b)w^2 \right] + O(t/Q^2) , \\ \mathcal{S}_{00}^{q\bar{q}} &= \frac{Q^2}{M_X^2 - t} \frac{1}{a} \{ 4K_1^2 (1 - 2w)^2 + 8K_2^2 w^2 \} + O(t/Q^2) , \\ \mathcal{S}_{+-}^{q\bar{q}} &= \frac{1}{a} \{ 8K_1^2 b (1 - w)^2 - 4K_2^2 b w (1 - w) \} + O(t/Q^2) , \end{aligned}$$

$$\mathcal{S}_{+0}^{q\bar{q}} = -4\sqrt{2} \frac{Q}{\sqrt{M_X^2 - t}} \frac{P_L \sqrt{M_X^2/4 - m_q^2 - P_L^2}}{M_X^2 - t} \frac{1}{a^2} \\ \left\{ K_1^2 (1-w)(1-2w) - K_2^2 w(1-2w)/2 \right\} + O(t/Q^2) . \quad (4.12)$$

For $t \rightarrow 0$ we recover our previous expressions (3.10), (3.16).

Let us now give some numerical examples, obtained with the parametrisation (4.8) of the integrals $I_i(t)$ which corresponds to the model gluon propagator (3.17) with $n = 4$. As in sec. 3.3 we change variables from P_L and $\varphi_{q\bar{q}}$ to $|P_L|$ and φ_{FB} and integrate over $|P_L|$. We impose an upper cutoff on $|P_L|$ and sum over the three light quark flavours u, d, s . In fig. 2 we plot the t -dependence of the quantities F_ε^{FB} , F_{00}^{FB} , F_{+-}^{FB} , F_{+0}^{FB} introduced in (3.19), but taking out the squared proton form factor $\tilde{G}^2(t)$ and the t -dependent part $\xi^{-2\alpha't}$ of the Regge power, both of which give a rather strong suppression of the cross section at t away from zero. As a result of the different t -behaviour of F_ε^{FB} , F_{+-}^{FB} and F_{+0}^{FB} the φ_{FB} -dependence of the ep cross section will change with t .

In order to see to what extent these results depend on the specific form of the gluon propagator we plot in fig. 3 the same quantities as in fig. 2, now with the simplest ansatz for the integrals we can make:

$$I_0(t) = \frac{9\beta_0^2}{4\pi} , \quad I_1(t) = \frac{9\beta_0^2}{4\pi} \frac{\mu_0^2}{2} , \quad I_2(t) = \frac{9\beta_0^2}{4\pi} |t| c_2^{(0)} , \quad (4.13)$$

keeping only the lowest order in t of the expansions (4.7). The leading coefficient $c_2^{(0)}$ in I_2 is not determined from phenomenology as is the case for I_0 and I_1 , and we take three different values 0, 0.5 and -0.5 . We see how the variation of $c_2^{(0)}$ modifies the behaviour of the Fourier coefficients at moderate and large values of $|t|$ quite drastically; it can for instance lead to a change of sign in the interference terms at fixed t . One would however have to see whether such large variations of $c_2^{(0)}$ can be obtained with realistic gluon propagators.

Comparing the plot for $c_2^{(0)} = 0$ and the corresponding one obtained with our special ansatz for the gluon propagator for which $c_2^{(0)} \approx 0$ we see that the effect of approximating the t -dependence of the integrals I_i by the leading terms in the expansions (4.7) is by no means small. This is not surprising as the leading order approximation is only expected to be good for $|t|/\mu_0^2 \ll 1$. Notice also that the first order coefficients $c_0^{(1)}$ and $c_1^{(1)}$ in (4.8) are rather large.

We have compared the results which include corrections up to order t/Q^2 with the expressions given in (4.12) where only the t -dependence through t/μ_0^2 in the integrals $K_i(t)$ is kept. In most of parameter space the latter give a very good approximation, and even for rather small Q^2 , M_X^2 or rather low minimum \mathbf{P}_T^2 the formulae (4.12) give the correct qualitative features. Apart of course from the squared elastic form factor $\tilde{G}(t)^2$ and the t -dependent pomeron trajectory the main effect in the t -dependence of the γ^*p cross sections and interference terms

thus turns out to be from the integrals $I_i(t)$, i.e. from the fact that at $t \neq 0$ the two exchanged gluons have different virtualities. On one hand this means that corrections in t/Q^2 are less important in the kinematical region we are investigating. On the other hand the results depend on the details of the nonperturbative gluon propagator encapsulated in the $I_i(t)$, and the phenomenological constraints (3.6), (3.7) are not sufficient to predict the t -dependence quantitatively, they only provide the right order of magnitude and the characteristic scale μ_0^2 .

5 The azimuthal angle of the scattered proton or proton remnant

In this section we turn our attention to another azimuthal angle in diffractive processes (2.1), choosing for the vector h

$$h = p_X \quad . \quad (5.1)$$

φ_X is the azimuthal angle between the lepton and the diffractive system X , i.e. $\varphi_X + \pi$ is the azimuthal angle between the lepton and the scattered proton or proton remnant. This angle was introduced and discussed in [9]. Note that the γ^*p cross sections and interference terms $\sigma_{mn}^{(X)}$ introduced there are integrated over the internal momenta of the system X but not over \tilde{p} . In the notation used in this paper they read

$$\sigma_{mn}^{(X)} \Big|_{\text{ref. [9]}} = \frac{1}{\pi} \frac{\beta}{\xi} \frac{d\sigma_{mn}^X}{d\beta dt} \Big|_{\text{this paper}} \quad . \quad (5.2)$$

p_X becomes collinear with q and p when $|t|$ takes its minimum value, which is zero in the high energy limit. As we remarked in sec. 2 the γ^*p interference terms must then vanish for $t \rightarrow 0$ because of angular momentum conservation, and the crucial question we will be concerned with in the following is how fast they do. To quantify this we normalise the interference terms with respect to the γ^*p cross sections and consider the ratios

$$\begin{aligned} R_{+-} &= \frac{d\sigma_{+-}^X/(d\beta dt)}{d\sigma_{++}^X/(d\beta dt) + d\sigma_{00}^X/(d\beta dt)} \quad , \\ R_{+0} &= \frac{d\sigma_{+0}^X/(d\beta dt)}{d\sigma_{++}^X/(d\beta dt) + d\sigma_{00}^X/(d\beta dt)} \quad . \end{aligned} \quad (5.3)$$

If they behave like a (possibly fractional) power of $|t|$ for $t \rightarrow 0$ then the scale that compensates t in these dimensionless quantities determines how large they are at finite t .

It was argued in [9] and confirmed by an explicit calculation in [22] that in the phenomenological pomeron model of Donnachie and Landshoff [23] one has

$$R_{+-} \sim \frac{|t|}{Q^2} \ , \qquad R_{+0} \sim \frac{\sqrt{|t|}}{Q} \ , \qquad (5.4)$$

where Q could be replaced by M_X or some combination of M_X and Q , the important point is that the scale dividing t is a kinematical quantity of the γ^*p subreaction, and therefore rather large compared with t for the typical values of t , M_X^2 and Q^2 in diffractive DIS.

For models that describe diffraction in terms of soft colour interactions [7, 8], or in models where the QCD vacuum plays an important role [24], one can expect a different behaviour [9]. In these models there is some scale characteristic of soft physics which could take the place of Q in the expressions of (5.4). This would lead to larger interference terms and thus to a more pronounced φ_X -dependence of the ep cross section. In the LN model the diffractive mechanism is described by soft gluon exchange; we will see in sec. 5.2 where and when its typical scale μ_0 replaces Q in (5.4). We remark that the powers of $|t|$ which give the small- t behaviour of R_{+-} and R_{+0} may in general be different from those in (5.4).

5.1 Calculation in the LN model

We now turn to the predictions of the LN model for the dependence of the ep cross section on the proton angle. We first have to replace the general diffractive final state X with a quark-antiquark pair. This is the lowest order approximation of X at parton level and should give a reasonable description, except in the region of small β , or large diffractive mass M_X , where additional gluon emission is known to be important.

The calculation of the γ^*p cross sections and interference terms for the process (3.1) is essentially the same as the one in sec. 4 with P of eq. (3.2) replaced by p_X in the expressions of the photon polarisation vectors (2.3). We integrate again over the relative azimuthal angle between \mathbf{P} and \mathbf{p}_X , but now the azimuthal angle between \mathbf{k} and \mathbf{p}_X is kept fixed, not the one between \mathbf{k} and \mathbf{P} .

We have to make an additional restriction on the diffractive final state, because we need that λ^2 of eq. (3.8), (4.4) is large for our approximations described in sec. 4.2 to be valid. Unless we have a large mass m_q for the produced quarks, this means that we must impose a lower cut on their transverse momentum.

In [9] it was shown that the γ^*p cross sections and interferences have a physical interpretation in terms of the helicity of the pomeron if one works in the rest frame of the diffractive system X , provided that the selection cuts on the hadronic final state are invariant when the particle momenta in the system X are rotated around the photon momentum in this frame while all other momenta are kept fixed. Nonzero interference terms between photons with definite helicities in

this frame imply that different amounts of angular momentum along the photon direction are transferred from the proton. In pomeron language this means that the pomeron can carry different helicities.

To satisfy the above criterion of rotation invariance we impose a cut on the transverse quark momentum in the X rest frame and not in the γ^*p system. To do this we have to transform the kinematical quantities introduced in sec. 3.1 to the c.m. of X . We denote three-momenta with an asterisk there and use a right-handed coordinate system with the z axis along the photon momentum \mathbf{q}^* . Both the transverse and the longitudinal momenta of the $q\bar{q}$ -pair are opposite to each other, not only the longitudinal ones as in the frame we used in sec. 3.1. Thus $\mathbf{P}^* = (\mathbf{P}_q^* - \mathbf{P}_{\bar{q}}^*)/2$ is equal to the three-momentum of the quark jet. Instead of χ and P_L of sec. 3.1 we use in the X rest system the relative azimuthal angle χ^* between \mathbf{P}^* and $\tilde{\mathbf{p}}^*$, and the longitudinal momentum P_L^* of $\mathbf{P}^* = \mathbf{P}_q^*$. Its kinematical limits are the same as for P_L . For the transverse component \mathbf{P}_T^* of \mathbf{P}^* in this system we have $\mathbf{P}_T^{*2} = M_X^2/4 - m_q^2 - P_L^{*2}$, compared with (3.3). The relation between the longitudinal and transverse components of P in both frames is as follows:

$$\begin{aligned} P_L &= \frac{1}{\sqrt{1 + 4\beta^2 t/Q^2}} \frac{M_X}{\sqrt{M_X^2 - t}} \left(P_L^* - |\mathbf{P}_T^*| \cos \chi^* \cdot (1 - 2\beta) \sqrt{-t}/M_X \right) , \\ |\mathbf{P}_T| \cos \chi &= -\frac{1}{\sqrt{1 + 4\beta^2 t/Q^2}} \left(|\mathbf{P}_T^*| \cos \chi^* + P_L^* \cdot (1 - 2\beta) \sqrt{-t}/M_X \right) , \\ |\mathbf{P}_T| \sin \chi &= -|\mathbf{P}_T^*| \sin \chi^* . \end{aligned} \quad (5.5)$$

Integrating over χ^* we obtain the ep cross section differential in φ_X , x , Q^2 , t , β and P_L^* . Note that P_L^* and χ^* are defined in the X rest frame, but φ_X in the γ^*p system.

5.2 Results

From our master formula (2.11) the φ_X -dependence of the ep cross section is given by the analogue of (3.9) in sec. 3.2, with the replacements $\varphi_{q\bar{q}} \rightarrow \varphi_X$, $P_L \rightarrow P_L^*$ and $d\sigma_{mn}^{q\bar{q}} \rightarrow d\sigma_{mn}^X$. The transverse-longitudinal interferences are real for the same reason as in the case of the jet angle. As in sec. 4.3 we have calculated the γ^*p cross sections and interference terms up to order t/Q^2 , treating t/μ_0^2 as of order 1. Again we will not give the analytic expressions of the $O(t/Q^2)$ terms, but use them in our numerical discussion. We find

$$\begin{aligned} \frac{d\sigma_{mn}^X}{dP_L^* d\beta dt} = & \frac{8}{3} \alpha_{em} e_q^2 \frac{\alpha_s(\lambda^{*2})}{\alpha_s^{(0)}} \tilde{G}^2(t) \xi^{2(1-\alpha_P(t))} \frac{1-\beta}{\beta M_X (M_X^2 + Q^2 - t)^2} \mathcal{S}_{mn}^X \end{aligned} \quad (5.6)$$

with

$$\begin{aligned}
\mathcal{S}_{++}^X &= \frac{K_1^2}{a^{*2}} \left[4(1-2a^*)b^*(1-w^*)^2 + (1-b^*)(1-2w^*)^2 \right] + \\
&\quad \frac{K_2^2}{a^{*2}} \left[(1-2a^*)b^*(1-2w^*+2w^{*2}) + 2(1-b^*)w^{*2} \right] + O(t/Q^2) , \\
\mathcal{S}_{00}^X &= \frac{Q^2}{M_X^2-t} \frac{1}{a^*} \left\{ 4K_1^2(1-2w^*)^2 + 8K_2^2 w^{*2} \right\} + O(t/Q^2) , \\
\mathcal{S}_{+-}^X &= \frac{8K_1K_2}{a^*} b^*(1-w^*)^2 + O(t/Q^2) , \\
\mathcal{S}_{+0}^X &= \frac{\sqrt{-2t}}{Q} \frac{Q^2}{M_X^2-t} \frac{1}{a^{*2}} \cdot \\
&\quad \left\{ K_1^2 \left[-(1-w^*)(1-7w^*+8w^{*2}) \right. \right. \\
&\quad \left. \left. + 4a^*(1-w^*)(1-8w^*+10w^{*2}) \right. \right. \\
&\quad \left. \left. + 2(1-4a^*)(1-\beta)(1-b^*)(1-6w^*+6w^{*2}) \right] \right. \\
&\quad \left. + K_1K_2 \left[-(1-w^*)(1-11w^*+16w^{*2})/2 \right. \right. \\
&\quad \left. \left. + 2a^*(1-w^*)(1-12w^*+20w^{*2}) \right. \right. \\
&\quad \left. \left. + (1-4a^*)(1-\beta)(1-b^*)(1-10w^*+12w^{*2}) \right] \right. \\
&\quad \left. + K_2^2 \left[w^*(2-9w^*+8w^{*2})/2 - 4a^*w^*(1-5w^*+5w^{*2}) \right. \right. \\
&\quad \left. \left. - 2(1-4a^*)(1-\beta)(1-b^*)w^*(1-3w^*) \right] \right\} \\
&\quad + O\left((-t/Q^2)^{3/2}\right) . \tag{5.7}
\end{aligned}$$

Here we have used the integrals $K_1(t)$, $K_2(t)$ introduced in (4.9), and the abbreviations

$$\begin{aligned}
b^* &= \frac{\mathbf{P}_T^{*2}}{\mathbf{P}_T^{*2} + m_q^2} , & w^* &= (1-\beta)b^* , \\
a^* &= \frac{\mathbf{P}_T^{*2} + m_q^2}{M_X^2} , & \lambda^{*2} &= \frac{\mathbf{P}_T^{*2} + m_q^2}{1-\beta} . \tag{5.8}
\end{aligned}$$

A remark is in order on the appearance of the square root $\sqrt{-t}$ in the expression of the transverse-longitudinal interference terms. One might suspect that there is a contradiction with the analyticity properties of scattering amplitudes, but this is not so. The point is that this interference term is multiplied with $\cos \varphi_X$ in the ep cross section, and that the expression of $\cos \varphi_X$ in terms of Mandelstam invariants also involves square roots, so that the appearance of $\sqrt{-t}$ is a consequence of the kinematical variables we choose. Put in a different way, the interference terms can have a dependence on $\sqrt{-t}$ through the polarisation vectors (2.3), which contain square roots. A corresponding remark can be

made for the appearance of P_L in the transverse-longitudinal interference term corresponding to the jet angle in (3.11), (4.12).

As discussed in sections 4.3 and 4.4 we have in the limit of small t

$$K_1(t) \xrightarrow{t \rightarrow 0} \frac{9\beta_0^2}{4\pi} \frac{\mu_0^2}{2} , \quad K_2(t) \xrightarrow{t \rightarrow 0} \frac{9\beta_0^2}{4\pi} |t| (c_2^{(0)} - 1/4) , \quad (5.9)$$

where $c_2^{(0)}$ is not known from phenomenology and has to be obtained using a specific ansatz for the nonperturbative gluon propagator. With (5.7) we find for the small- t behaviour of the interference terms normalised to the γ^*p cross sections

$$R_{+-} \sim (c_2^{(0)} - 1/4) \frac{|t|}{\mu_0^2} , \quad R_{+0} \sim \frac{\sqrt{|t|}}{Q} . \quad (5.10)$$

Note that the behaviour of \mathcal{S}_{+-}^X in the limit $t \rightarrow 0$ is determined by the coefficient $c_2^{(0)}$, in contrast to the case of the jet angle investigated in sec. 4.4, where we could make a parameter-free prediction for this limit. In particular the sign of the transverse-transverse interference depends on the details of the gluon propagator. If $c_2^{(0)}$ is close to $1/4$ one even finds that the $O(t/Q^2)$ terms are dominant and $R_{+-} \sim |t|/Q^2$. Apart from this caveat the result (5.10) is however independent of the detailed properties of the gluon propagator. The scale μ_0^2 comes into play in this model via the nonperturbative dynamics of the exchanged gluons. Since it only appears squared in the calculation, cf. (4.7), it is clear that it can not be the scale dividing $\sqrt{-t}$ in R_{+0} ; there we have the large kinematical variable Q as in (5.4).

The situation is however more complicated for R_{+-} than discussed so far. We will not find ratios R_{+-} of order one as suggested by (5.10) in our numerical examples. The reason is that \mathcal{S}_{+-}^X (but not \mathcal{S}_{+0}^X) has an additional suppression compared with the cross section term \mathcal{S}_{++}^X by a factor of $a^*b^* = \mathbf{P}_T^{*2}/M_X^2$, which can be rather small for the \mathbf{P}_T^{*2}/M_X^2 where we cut in the case of light quarks, and even goes down to zero for charm production. After integration over \mathbf{P}_T^{*2} the first relation of (5.10) is more precisely

$$R_{+-} \sim (c_2^{(0)} - 1/4) \frac{|t|}{\mu_0^2} \cdot \frac{\mathbf{P}_{Tcut}^{*2}}{M_X^2} , \quad (5.11)$$

for light quarks with a momentum cutoff and

$$R_{+-} \sim (c_2^{(0)} - 1/4) \frac{|t|}{\mu_0^2} \cdot \frac{m_q^2}{M_X^2} , \quad (5.12)$$

for heavy quarks and integration down to $\mathbf{P}_T^{*2} = 0$. In (5.12) m_q^2 appears since it is the typical scale of \mathbf{P}_T^{*2} in the integration if the quark mass is large.

The question arises what one can expect for R_{+-} when there is no lower cut on \mathbf{P}_T^{*2} in the case of light quarks. After all the main contribution to $d\sigma_{mn}^X/(dt d\beta)$

summed over all flavours and the full phase space is from light quarks at low transverse momenta. Because of the approximations of our calculation we cannot extrapolate (5.7) to this region, but we want to give an educated guess. We have argued in [6, 25] that with some caveats the LN model can still be applied to $\gamma^* p \rightarrow q\bar{q}p$ in the limit $\mathbf{P}_T^{*2} + m_q^2 \rightarrow 0$. In the results (3.11) from our investigation of the jet angle dependence at $t = 0$ we observe that the suppression of $\mathcal{S}_{+-}^{q\bar{q}}$ with respect to $\mathcal{S}_{++}^{q\bar{q}}$ is by a factor \mathbf{P}_T^2/M_X^2 even in this limit. Taking this as a guidance for the interference term in our present problem we expect that a suppression by \mathbf{P}_T^2/M_X^2 of the differential interference term may persist for very small $\mathbf{P}_T^{*2} + m_q^2$, so that \mathbf{P}_{Tcut}^{*2} in (5.11) is to be replaced with some average \mathbf{P}_T^{*2} if we integrate over the full phase space. Examining the loop integrals $L_i(\mathbf{P}_T^2, w)$ of (3.12) one further finds that the typical scale for the \mathbf{P}_T^2 -dependence of the cross section is μ_0^2 in the case where m_q^2 is small and β not too close to 1. This leads us to the guess

$$R_{+-} \sim (c_2^{(0)} - 1/4) \frac{|t|}{\mu_0^2} \cdot \frac{\mu_0^2}{M_X^2} \sim \frac{|t|}{Q^2} \quad (5.13)$$

for the interference term without a cut on \mathbf{P}_T^{*2} , which is the quantity originally discussed in [9]. Notice that the $O(t/Q^2)$ terms in \mathcal{S}_{+-}^X now also contribute to the leading term of R_{+-} . The scale μ_0^2 has cancelled and we find the same behaviour for both R_{+-} and R_{+0} as in the Donnachie Landshoff model (5.4). Let us however remark that there one has $R_{+-} \sim |t|/Q^2$ even with a large cutoff on \mathbf{P}_T^{*2} , in contrast to (5.10), (5.11), so that the predictions of the two models are by no means identical.

Coming back to what we were able to calculate in the LN model we now give some numerical illustrations of our results. In analogy to sec. 4.4 we integrate over P_L^* and plot the Fourier coefficients F_ε^X , F_{+-}^X , F_{+0}^X with a global factor $\tilde{G}^2(t) \xi^{-2\alpha' t}$ taken out. They are defined like F_ε^{FB} , F_{+-}^{FB} , F_{+0}^{FB} in (3.19) with the superscript FB replaced by X and thus appear in $d\sigma(ep \rightarrow epq\bar{q})/(d\varphi_X dx dQ^2 d\beta dt)$ in a manner analogous to (3.20). We either sum over the three light flavours u, d, s for the produced quarks, with a minimum \mathbf{P}_T^{*2} so that our calculation is valid, or we consider produced charm quarks for which we can integrate over the full kinematical range of P_L^* .

The t -dependence of the Fourier coefficients for the model propagator (3.17) with $n = 4$ is shown in fig. 4 for different values of the free kinematical parameters. We observe that the transverse-transverse interference is usually larger than the transverse-longitudinal one. Fig. 5 shows an example of the φ_X -dependence of the ep cross section at two different values of t . In case (b) the distribution is clearly not flat, although the effect is not very large, whereas in case (a) almost no φ_X -dependence can be seen. This illustrates how the transverse-transverse interference is affected by the parameter $\mathbf{P}_{Tcut}^{*2}/M_X^2$, which is $1/20$ in case (a) and $1/5$ in case (b).

To assess the model dependence of our prediction we also evaluated the Fourier

coefficients taking the simple ansatz (4.13) for the integrals over the gluon propagators, with different values for the coefficient $c_2^{(0)}$. They are shown in fig. 6 for the case of light quarks, the effects for charm are similar. As in sec. 4.4 the results, especially at large $|t|$, change considerably with $c_2^{(0)}$. In particular the sign of the transverse-transverse interference term is different for $c_2^{(0)}$ below or above $1/4$, and for $c_2^{(0)} = 1/4$ this term is very small, as discussed above. We repeat that one would have to see whether realistic gluon propagators give values of $c_2^{(0)}$ as far away from zero as the ones taken in fig. 6.

We find that the leading order expressions of \mathcal{S}_{++}^X , \mathcal{S}_{00}^X and \mathcal{S}_{+-}^X in (5.7) give a rather good approximation of what is obtained by including terms of $O(t/Q^2)$, except of course for \mathcal{S}_{+-}^X if $c_2^{(0)} = 1/4$. As in sec. 4.4 this means that the main effect comes from terms depending on t/μ_0^2 , whereas corrections in t/Q^2 are relatively small. Terms in t/μ_0^2 are also essential to describe the t -dependence of \mathcal{S}_{+0}^X . Although its order of magnitude at small t is given by $\sqrt{-t}/Q$, a mere square root dependence on $|t|$ for the Fourier coefficient F_{+0}^X in figures 4 and 6 is clearly not a good approximation unless t is very small.

To conclude this section we remark on the possibility to constrain the cross section for longitudinal photons from the measurement of the φ_X -dependence using the method described in sec. 2.1. With the results we obtain in the LN model the bounds on $d\sigma_{00}/(dt d\beta)$ would not be stringent at all, and be far away from its actual value. This is because we find the interference $d\sigma_{+0}/(dt d\beta)$, whose size is crucial to obtain good constraints, to be of order $\sqrt{|t|}/Q$. From (2.16) we can see that the lower bound on $d\sigma_{00}/(dt d\beta)$ then vanishes like $|t|/Q^2$ for small t , whereas $d\sigma_{00}/(dt d\beta)$ itself does not become small in this limit. This is different from the situation we found for the jet angle in sec. 3.3. One would expect better bounds if the ratio of the longitudinal-transverse interference and the γ^*p cross sections at small t were dominated by a hadronic scale instead of Q or M_X . This might happen in other models of diffraction where soft dynamics is important.

6 Summary

In this paper we investigated correlations between azimuthal angles in deep inelastic ep diffraction, using the one-photon approximation. We first derived the general expression for the dependence of the ep cross section on a suitably defined azimuthal angle between the lepton plane and a direction in the hadronic final state in terms of cross sections and interference terms of the γ^*p collision for different photon helicities. This was a direct generalisation of the work in [9]. We showed that those terms in the cross section that depend on the helicity of the lepton beam are sensitive to a polarisation dependence of the phases in the γ^*p amplitudes for linearly polarised photons. From the angular dependence of the ep cross section one can obtain bounds on the differential or integrated cross

section for longitudinal photons, without having to vary y as it is needed for its direct measurement. How stringent these bounds are depends on the size of the interference term between longitudinal and transverse polarisations and thus on the choice of azimuthal angle and on the region of phase space considered.

We have investigated the dependence on the azimuthal jet angle predicted by the LN model for the parton level reaction $ep \rightarrow ep + q\bar{q}$ at large transverse momentum of the $q\bar{q}$ -pair, which at hadron level describes a pair of jets that carries the entire four-momentum of the diffractive final state. The size of the interference terms is found to be controlled by the quantity \mathbf{P}_T^2/M_X^2 . The sign of the transverse-longitudinal interference depends on β . Since this interference is less strongly suppressed than the longitudinal cross section, it may offer an opportunity to observe the zero of the longitudinal amplitude at certain values of \mathbf{P}_T^2 and β which is characteristic of the two-gluon exchange mechanism. The bounds on the longitudinal cross section obtained from the azimuthal dependence might be quite useful, at small \mathbf{P}_T^2/M_X^2 at least the lower bound comes out quite close to its actual value which is also small in this kinematical region. We suggest that the use of an azimuthal angle defined from an event shape variable like the thrust axis in the diffractive final state would allow to extend this method to a wider class of final states, in particular it would allow to go to smaller values of \mathbf{P}_T^2 than those needed for jet algorithms and thus to increase the total rate in the analysis.

The cross section for $ep \rightarrow ep + q\bar{q}$ was then calculated at finite t with the approximations $\Delta_T^2 \ll \lambda^2$ and $\mathbf{I}_T^2 \ll \lambda^2$, for the definition of λ^2 cf. (3.8), (4.4). Its region of validity is therefore the production of jets or heavy flavours where λ^2 is sufficiently large. The result then involves three t -dependent integrals (4.6) with two gluon propagators at different virtualities. The relevant scale for the t -behaviour of these integrals is $\mu_0^2 \approx 1.2 \text{ GeV}^2$. The limit $t \rightarrow 0$ for two of them is known from phenomenology, for the rest one has to resort to specific model propagators.

Applying this calculation to the dependence on the azimuthal jet angle we find that apart from the dominating effect of the proton form factor $\tilde{G}(t)$ and the pomeron trajectory $\alpha_P(t)$ the t -dependence of the γ^*p cross sections and interference terms is controlled by corrections in t/μ_0^2 coming from the gluon propagators, corrections in t divided by a large kinematical scale of the transition $\gamma^* \rightarrow q\bar{q}$ are much smaller. As a consequence the quantitative features of the results depend on the choice of gluon propagator. Using the model propagator (3.17) we typically find that the sum of the transverse and longitudinal cross sections decreases by a factor around 2 between $|t| = 0$ and 1.4 GeV^2 when the strong suppression from $\tilde{G}(t)$ and the pomeron trajectory is taken out. The absolute size of the interference terms tends to decrease with $|t|$ and one can even have a change of their signs.

Another important azimuthal angle is that of the scattered proton or proton remnant. It was shown in [9] that its measurement can give information on the

helicity structure of the pomeron. We have investigated its distribution in the LN model, but due to our approximations had to restrict ourselves to a $q\bar{q}$ final state with large transverse quark momentum \mathbf{P}_T^* in the $q\bar{q}$ rest frame, or with a large quark mass. Like for the jet angle we find that the t -dependence of the cross sections and interference terms is controlled by the scale μ_0^2 , and that the results depend rather strongly on the integrals over the gluon propagators. The order of magnitude of the transverse-longitudinal interference is given by $\sqrt{-t}/Q$. The ratio between the interference of the two transverse polarisations and the transverse cross section goes like t/μ_0^2 which can be large, but it is suppressed by an additional factor \mathbf{P}_T^{*2}/M_X^2 so that this interference is small at low \mathbf{P}_T^{*2} . Unfortunately we cannot take the limit $\mathbf{P}_T^{*2} \rightarrow 0$ for light quarks in our calculation but our guess is that the \mathbf{P}_T^{*2} -integrated transverse-transverse interference will be suppressed by t/Q^2 compared with the transverse cross section, which would lead to a rather flat angular dependence in the ep spectrum. According to the discussion in [9] the helicity of the LN pomeron is then dominated by one value in the inclusive diffractive process, whereas several helicities are important when there is a high transverse momentum or mass scale in the diffractive final state. Notice that a system of two gluons we use to model the pomeron can in principle transfer any integer value of angular momentum through its orbital motion.

Our finding that finite- t effects are rather sensitive to the nonperturbative gluon dynamics in the LN model suggests that they may come out quite different in other models of diffraction and could thus be a useful probe of the mechanisms at work in diffractive physics.

Acknowledgements

I wish to thank O. Nachtmann and P. V. Landshoff for numerous discussions, and O. Nachtmann and B. Pire for valuable remarks on the manuscript. I gratefully acknowledge conversations with T. Arens, J. Bartels, H. Jung, H. Lotter, N. Pavel and H. Pirner.

This work was supported by the ARC Programme of the British Council and the German Academic Exchange Service, grant 313-ARC-VIII-VO/scu, and by the EU Programme “Human Capital and Mobility”, Network “Physics at High Energy Colliders”, Contracts CHRX-CT93-0357 (DG 12 COMA) and ERBCHBI-CT94-1342. It was also supported in part PPARC.

References

- [1] ZEUS Collaboration, Phys. Lett. B 315 (1993) 481;
H1 Collaboration, Nucl. Phys. B429 (1994) 477
- [2] G Ingelman and P Schlein, Phys. Lett. B 152 (1985) 256

- [3] N N Nikolaev and B G Zakharov, Z. Phys. C 53 (1992) 331
- [4] J Bartels, H Lotter and M Wüsthoff, Phys. Lett. B 379 (1996) 239;
M Wüsthoff, Ph. D. thesis, Univ. of Hamburg, DESY 95-166
- [5] J Bartels and M Wüsthoff, Z. Phys. C 66 (1995) 157;
E Levin and M Wüsthoff, Phys. Rev. D 50 (1994) 4306
- [6] M Diehl, Z. Phys. C 66 (1995) 181
- [7] W Buchmüller and A Hebecker, Phys. Lett. B 355 (1995) 573; Nucl. Phys. B476 (1996) 203
- [8] A Edin, G Ingelman and J Rathsman, Phys. Lett. B 366 (1996) 371
- [9] T Arens, M Diehl, P V Landshoff and O Nachtmann, hep-ph/9605376, to appear in Z. Phys. C
- [10] T Gehrmann and W J Stirling, Z. Phys. C 70 (1996) 89
- [11] J Bartels, C Ewerz, H Lotter and M Wüsthoff, Phys. Lett. B 386 (1996) 389
- [12] P V Landshoff and O Nachtmann, Z. Phys. C 35 (1987) 405
- [13] M Gourdin, Il Nuovo Cimento 21 (1961) 1094;
C W Akerlof et al., Phys. Rev. Lett. 14 (1965) 1036;
H Georgi and H D Politzer, Phys. Rev. Lett. 40 (1978) 3;
A Méndez, A Raychaudhuri and V J Stenger, Nucl. Phys. B148 (1979) 499;
R N Cahn, Phys. Lett. B 78 (1978) 269; Phys. Rev. D 40 (1989) 3107;
E L Berger, Phys. Lett. B 89 (1980) 241;
V Hedberg, G Ingelman, C Jacobsson and L Jönsson, “Asymmetries in jet azimuthal angle distributions as a test of QCD”, in: *Physics at HERA*, eds. W Buchmüller and G Ingelman, DESY, 1992, p. 331;
J Chay, S D Ellis and W J Stirling, Phys. Rev. D 45 (1992) 46;
R Meng, F I Olness and D E Soper, Nucl. Phys. B371 (1992) 79
- [14] G Köpp, R Maciejko and P M Zerwas, Nucl. Phys. B144 (1978) 123
- [15] L Hand, Phys. Rev. 129 (1963) 1834
- [16] A Donnachie and P V Landshoff, Nucl. Phys. B311 (1988/89) 509
- [17] J M Cornwall, Phys. Rev. D 26 (1982) 1453;
D Zwanziger, Nucl. Phys. B323 (1989) 513;
K Büttner and M R Pennington, Phys. Lett. B 356 (1995) 354; Phys. Rev. D 52 (1995) 5220;
D S Henty, C Parrinello and D G Richards, Phys. Lett. B 369 (1996) 130

- [18] J R Cudell, A Donnachie and P V Landshoff, Nucl. Phys. B322 (1989) 55
- [19] M Genovese, N N Nikolaev and B G Zakharov, Phys. Lett. B 378 (1996) 347
- [20] J Bartels, C Ewerz, H Lotter, M Wüsthoff and M Diehl, “Quark-antiquark jets in DIS diffractive dissociation”, hep-ph/9609239, in: *Future Physics at HERA*, Proc. of the workshop 1995/96, eds. G Ingelman, A De Roeck and R Klanner, DESY 1996
- [21] M G Ryskin, Z. Phys. C 57 (1993) 89;
S J Brodsky et al., Phys. Rev. D 50 (1994) 3134
- [22] M Diehl, “Diffraction in electron-positron collisions”, Ph. D. thesis, Univ. of Cambridge, 1996 (unpublished)
- [23] A Donnachie and P V Landshoff, Phys. Lett. B 191 (1987) 309; Nucl. Phys. B303 (1988) 634; Phys. Lett. B 185 (1987) 403
- [24] O Nachtmann and A Reiter, Z. Phys. C 24 (1984) 283;
A Brandenburg, E Mirkes and O Nachtmann, Z. Phys. C 60 (1993) 697;
G W Botz, P Haberl and O Nachtmann, Z. Phys. C 67 (1995) 143;
O Nachtmann, “The QCD vacuum structure and its manifestations”, in: *Confinement Physics*, Proc. of the First ELFE Summer School, Cambridge, UK, 22–28 July 1995, eds. S D Bass and P A M Guichon, Editions Frontières, Gif-sur-Yvette 1996
- [25] M Diehl, hep-ph/9701252

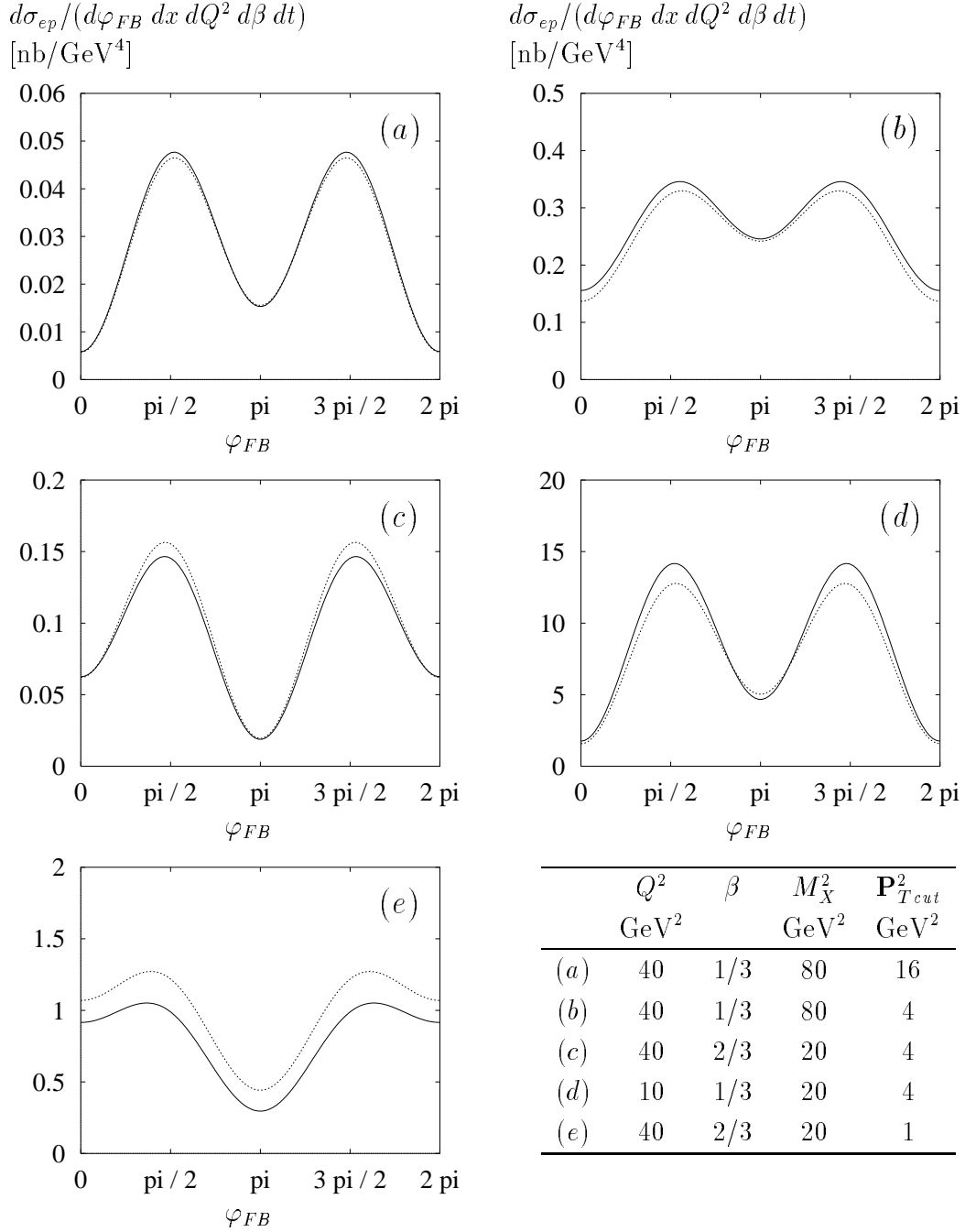


Figure 1: Dependence on φ_{FB} of $d\sigma(ep \rightarrow epq\bar{q})/(d\varphi_{FB} dx dQ^2 d\beta dt)$, summed for u, d, s and c quarks. Values of the free kinematical variables are $\sqrt{s} = 296$ GeV, $y = 0.5$, $\varepsilon = 0.8$, $t = 0$ and those given in the table. A cut $\xi \leq 0.05$ has been imposed. Full lines correspond to the improved approximation (3.18) of (3.11), dotted ones to the simplified results (3.16) obtained with the approximation (3.15).

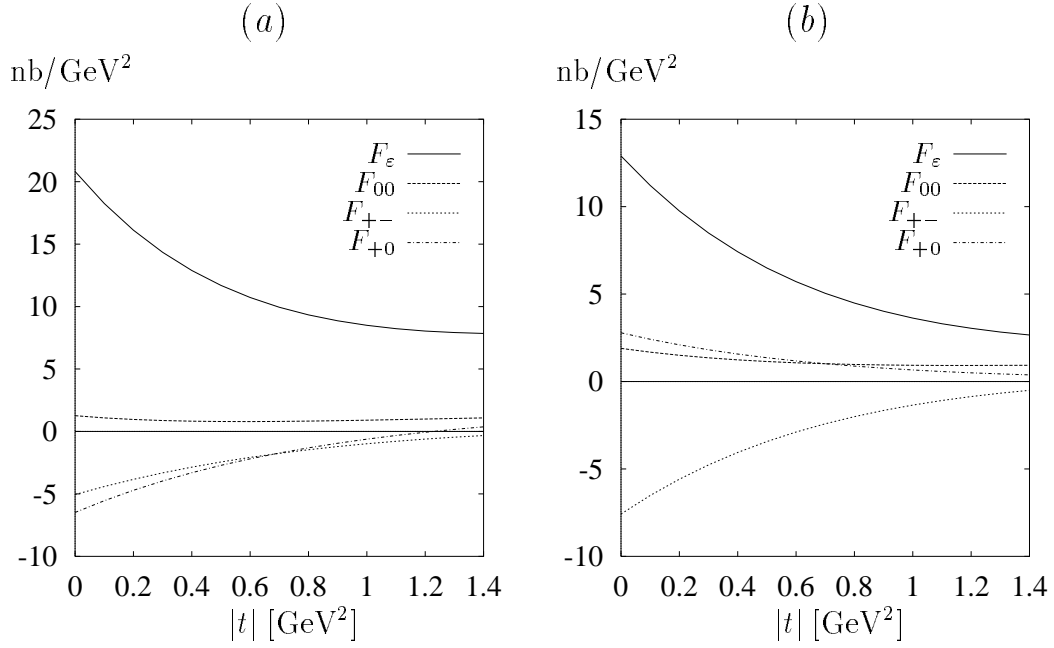


Figure 2: Fourier coefficients F_ε^{FB} , F_{+-}^{FB} , F_{+0}^{FB} in the ep cross section and the contribution F_{00}^{FB} of longitudinal photons to F_ε^{FB} . For their definition cf. (3.19). They are summed for u, d, s quarks and a global factor $\tilde{G}^2(t) \xi^{-2\alpha't}$ is taken out in the plot. The results here are obtained with the model gluon propagator (3.17) for $n = 4$. Kinematical variables are (a): $\sqrt{s} = 296$ GeV, $y = 0.5$, $Q^2 = 40$ GeV², $\beta = 1/3$, $|P_L| \leq 4$ GeV. (b): \sqrt{s} and y as before and $Q^2 = 40$ GeV², $\beta = 2/3$, $|P_L| \leq 1$ GeV.

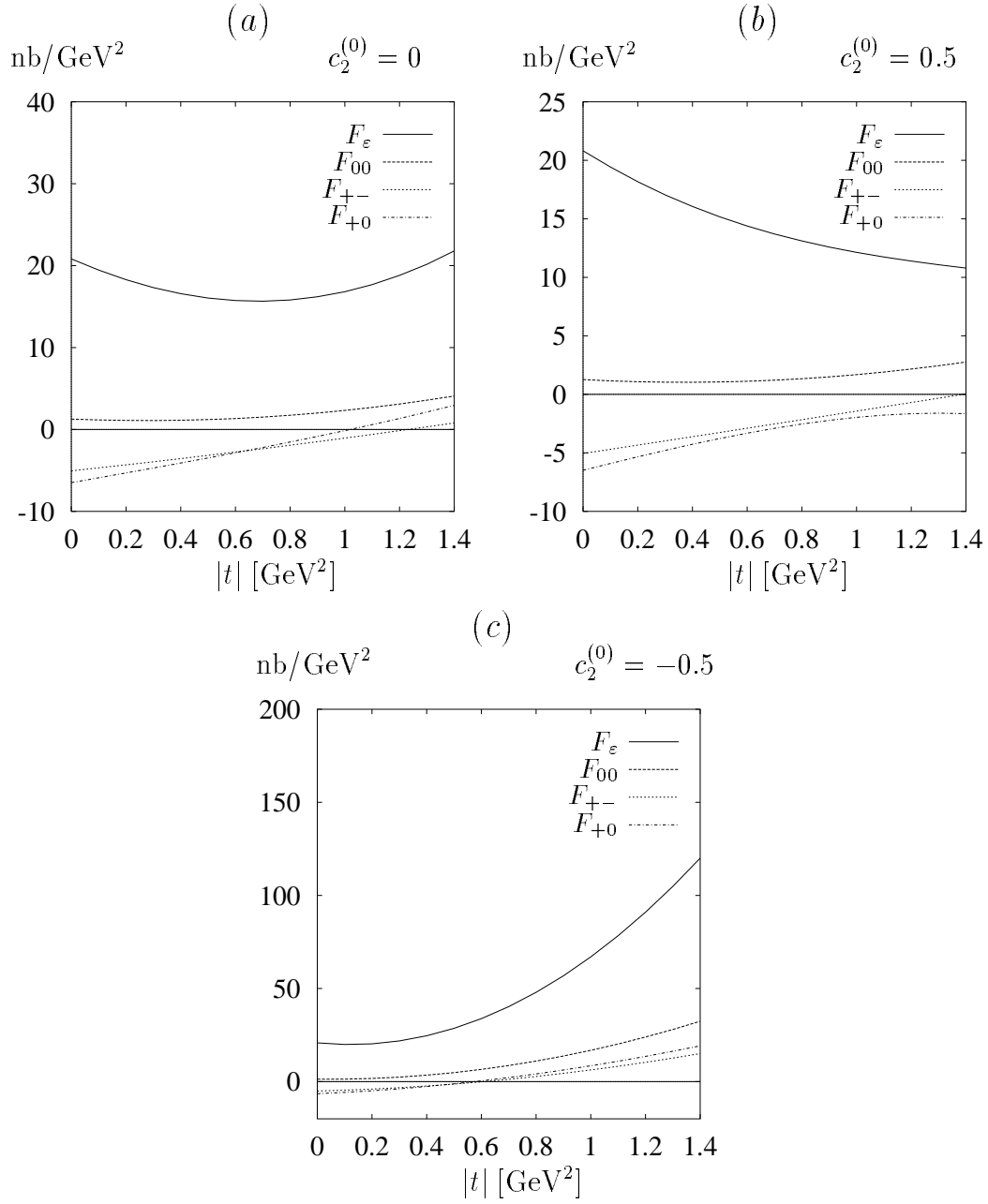


Figure 3: As fig. 2 (a) but with the ansatz (4.13) for the integrals over the gluon propagators with different values of $c_2^{(0)}$. Remember that a factor $\tilde{G}^2(t) \xi^{-2\alpha t}$ is taken out in the plot; the differential cross section does not rise with $|t|$.

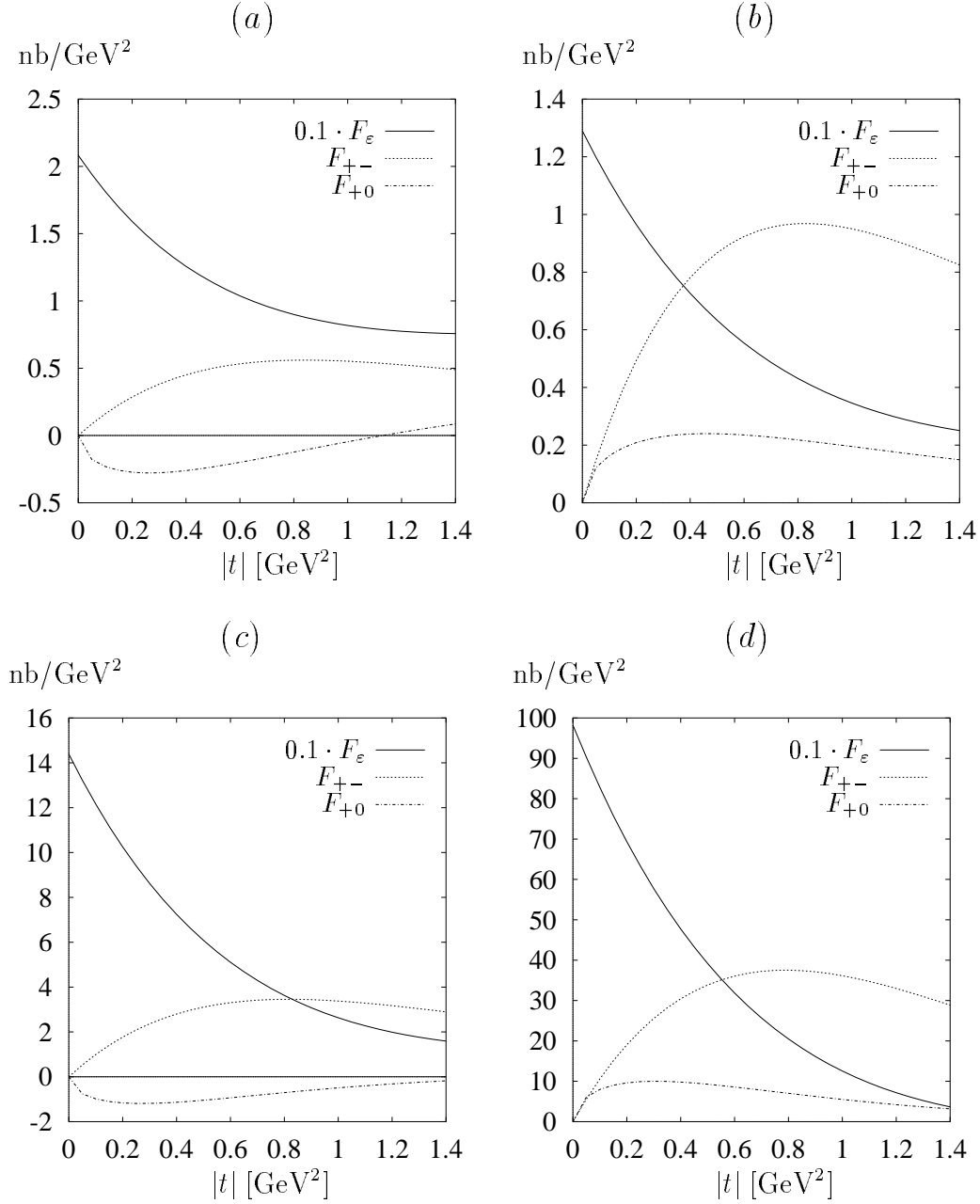


Figure 4: Fourier coefficients F_ε^X , F_{+-}^X , F_{+0}^X in the ep cross section, defined in analogy to (3.19), with a global factor $\tilde{G}^2(t) \xi^{-2\alpha' t}$ taken out. Note that F_ε^X is scaled down by a factor 10. (a) and (b) are summed for u, d, s quarks with a lower cutoff $\mathbf{P}_T^{*2} \geq 4 \text{ GeV}^2$, (c) and (d) are for charm quarks without a cut on \mathbf{P}_T^{*2} . Kinematical variables are $\sqrt{s} = 296 \text{ GeV}$, $y = 0.5$ in all cases and (a): $Q^2 = 40 \text{ GeV}^2$, $\beta = 1/3$. (b): $Q^2 = 40 \text{ GeV}^2$, $\beta = 2/3$. (c): $Q^2 = 25 \text{ GeV}^2$, $\beta = 1/3$. (d): $Q^2 = 6.25 \text{ GeV}^2$, $\beta = 1/3$. The curves are obtained with the model gluon propagator (3.17) with $n = 4$.

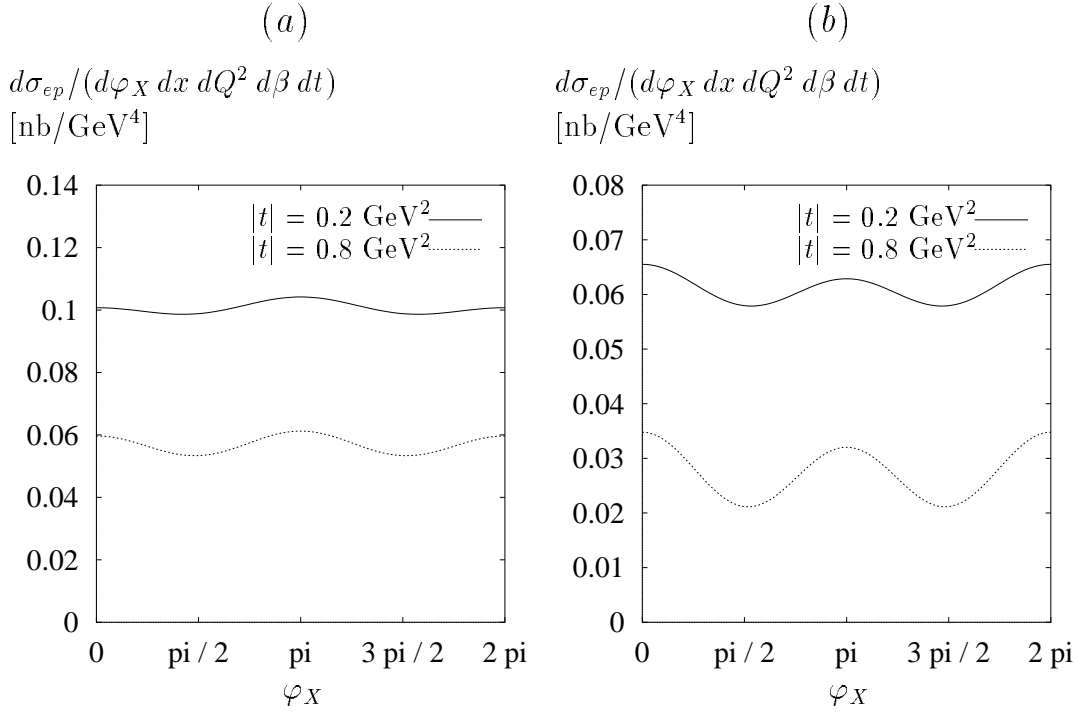


Figure 5: (a): Dependence on φ_X of $d\sigma(ep \rightarrow ep q\bar{q})/(d\varphi_X dx dQ^2 d\beta dt)$, obtained from the Fourier coefficients in fig. 4 (a) for $|t| = 0.2 \text{ GeV}^2$ and $|t| = 0.8 \text{ GeV}^2$. (b): The same for the Fourier coefficients from fig. 4 (b)

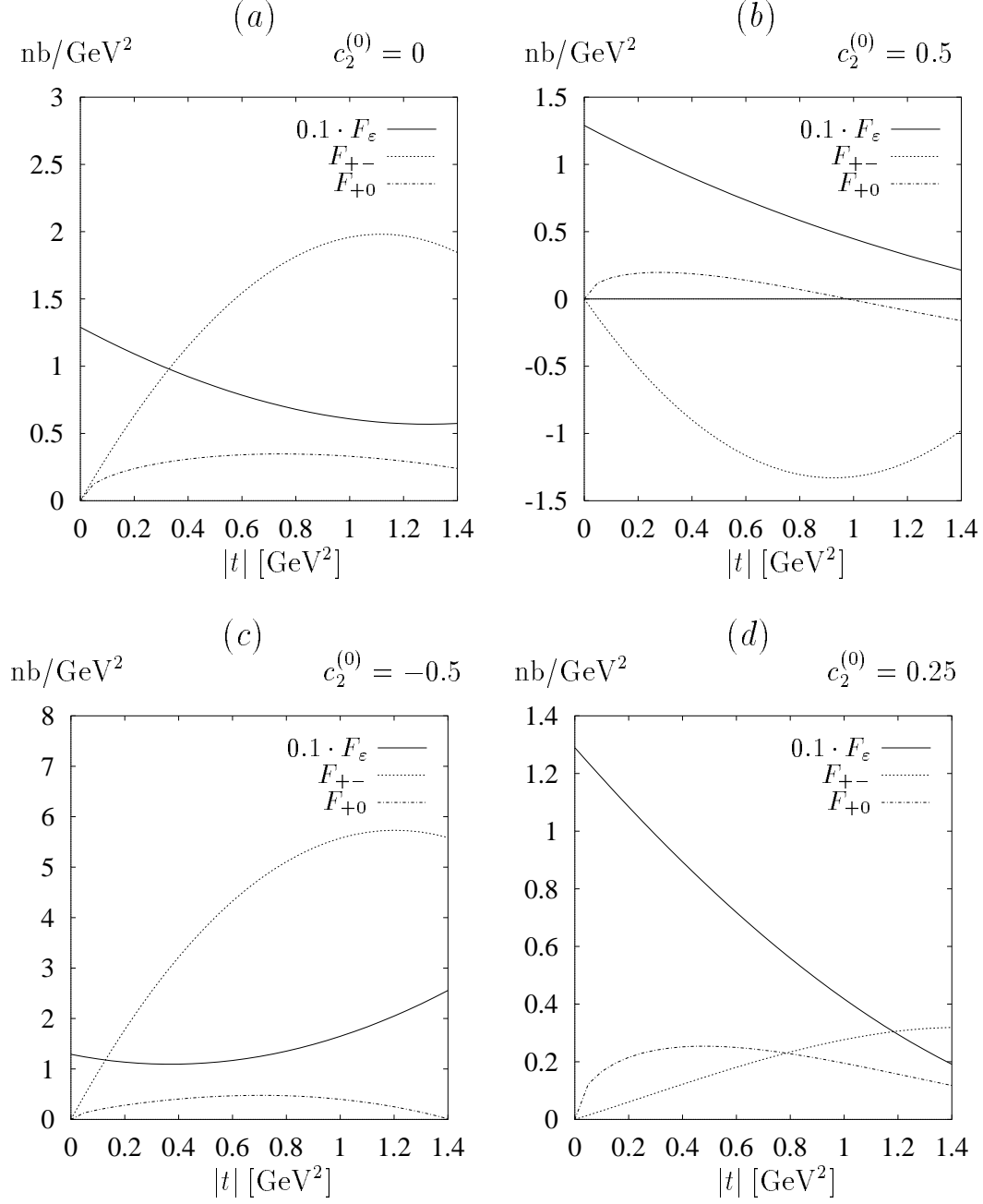


Figure 6: As fig. 4 (b), but with the ansatz (4.13) for the integrals over the gluon propagators with different values of $c_2^{(0)}$.